International Atomic Energy Agency

INDC(NDS)-287

INDC INTERNATIONAL NUCLEAR DATA COMMITTEE

An Evaluated Data Base for Sputtering

E.W. Thomas*, R.K. Janev, J. Botero, J.J. Smith and Yanghui Qiu#

International Atomic Energy Agency

P.O. Box 100

A-1400 Vienna, Austria

October 1993

* Permanent address: School of Physics, Georgia Institute of Technology, Atlanta Georgia 30332-0430, USA

Permanent address: Institute of Applied Physics and Computational Mathematics, P.O. Box 8009, Beijing 100088, People's Republic of China

IAEA NUCLEAR DATA SECTION, WAGRAMERSTRASSE 5, A-1400 VIENNA

INDC(NDS)-287

An Evaluated Data Base for Sputtering

E.W. Thomas*, R.K. Janev, J. Botero, J.J. Smith and Yanghui Qiu#

International Atomic Energy Agency

P.O. Box 100

A-1400 Vienna, Austria

October 1993

* Permanent address: School of Physics, Georgia Institute of Technology, Atlanta Georgia 30332-0430, USA

Permanent address: Institute of Applied Physics and Computational Mathematics, P.O. Box 8009, Beijing 100088, People's Republic of China

Abstract

Previously published data on physical sputtering of surfaces by light ions are critically reviewed with the aim of providing a single evaluated data set for a range of projectile-target combinations of interest to the modelling of plasma fusion device's first wall interactions. Experimental data often exhibits poor reliability and are not necessarily suitable for testing empirical formulae. Moreover, previously published empirical formulae are shown to be inconsistent with recent Monte-Carlo simulations. A revised set of formulae is suggested with empirical constants evaluated by comparison with the simulation data and is shown to be consistent with experiment. Fitting of the proposed formulae to an experimental data for a specific projectile target combination can be achieved with a single parameter.

Reproduced by the IAEA in Austria
October 1993

93-03954

1. INTRODUCTION

We consider the available data for light atomic particle sputtering of surfaces with the objective of establishing a base of reliable data and developing an algebraic representation based on the systematics of behaviour. Sputtering of surfaces is an important parameter in the understanding of fusion energy device operation. Sputtering ejects high atomic number materials into the plasma causing significant contamination, rise in the effective Z of the plasma and inefficient heating of the fuel. To assist with the understanding and modelling of plasma device operation we seek to provide a base of reliable sputtering data with an algebraic representation that may be conveniently incorporated into plasma modelling codes. With our particular interest in fusion related applications we will restrict our discussions to sputtering of polycrystalline candidate plasma facing component materials by light ions (H^+, D^+, T^+, He^+) at energies from a few times 10 eV, characteristic of acceleration through the plasma sheath, to several tens of keV, that might be appropriate to neutral beams used for large tokamak plasma heating and diagnostics.

The sputtering yield (or coefficient) is given the symbol $Y(E_o)$ and is defined as the total number of target atoms ejected for every projectile atom incident at energy E_o. For the present work we restrict ourselves to normal incidence of projectiles with the ejected atoms integrated over all emerging trajectories, energies, charge and quantum states. It is only for these conditions that there is a large experimental data base against which we might test algebraic representations of data.

We confine ourselves to the process of physical sputtering where the ejection mechanism relates to collisional transfer of kinetic energy and momentum from the projectile to target atoms. Such a process will be largely independent of the target temperature. We will not be considering chemical sputtering, i.e. where a projectile comes to (nominal) rest in the solid, combines with a target atom, and then is thermally released, or radiation enhanced sublimation (RES). These processes are very well known for the erosion of carbon by hydrogen where the volatile species are hydrocarbons; this type of erosion process is temperature dependent.

Sputtered particles generally eject from the first one or two surface layers. To eject there must be an energy transferred to the target atom which exceeds the binding energy of that atom to the solid. As a result there will be a finite threshold of projectile energy below which no ejection will take place; the threshold will be related to the masses of the colliding species and the precise nature of the ejection mechanism. For heavy projectiles ejection occurs primarily as a result of a series of collisions between recoiling target atoms in the collision cascade; this will be related to nuclear stopping. For light projectiles the backscattering of the projectile from some depth in the solid may be quite significant and as the reflected projectile returns to the surface it may eject a surface atom by a head-on collision. Thus for light projectiles that we are considering here the ejection is related not only to the energy deposited in the collision cascade close to the surface but also to the reflection of the projectile from the solid. Sputtering yields due to light projectile impact generally peak at 1 to 10 keV projectile energy with a magnitude of 10^{-1} to 10^{-3} (target atoms ejected per projectile atom). As projectile energy increases beyond the maximum for Y, the ejection decreases due to reduction of the projectile reflection coefficients and also to reduction of the energy deposited in the near surface collision cascade (related to nuclear stopping power). As projectile energy decreases from the yield peak, Y will decrease becoming zero at a finite threshold related to binding energy; these thresholds are generally in the 10 to 200 eV region.

Theoretical predictions of sputtering are limited to generalized formulations with various unknown coefficients that must be established by comparison with some other data. The question of near-threshold behaviour has received no detailed treatment at all. Monte Carlo simulation calculations are available for many cases of interest to the present study and are consistent with experiment to within the combined accuracy limits. While these do require the input of theoretical parameters such as binding energy and potentials, these parameters can be validated by reference to subsidiary data. The results of simulations appear to be quite reliable. Experiments are generally performed by measuring the weight loss of the target as a result of particle bombardment. Results are available for most of the cases of interest here although often restricted to a small range of energies close to the yield peak where signals are high and measurements are

relatively easy. Experimental data is often of poor statistical accuracy and may suffer systematic errors due to calibration difficulties and the presence of surface contaminants.

We approach this problem from the point of view that the Monte Carlo simulations, where they exist, are likely to provide the most reliable numerical data. We take the generalized theoretical predictions of sputtering as a guide for the construction of algebraic expressions to represent sputtering yield. These will be compared with simulations to establish unknown parameters. The result will then be compared with available experiment to validate both the simulation and the derived parameters. We show that the relative variation of yield with projectile energy can be well represented in this manner with a limited set of general parameters. The final step is the evaluation of a single normalizing constant to establish absolute magnitude for each collision case; this is derived by comparison with experiment. In the few cases where there is no experimental data (particularly for T^+ ions which have never been studied directly) we expect to establish the final normalizing constant by interpolation between data sets for similar collision combinations. The result of this procedure is an algebraic expression to represent each case of collision partners of interest that may be used to create data tables and graphs for reference or may be used directly in a fusion plasma device modelling program. These expressions are consistent with the Monte Carlo simulations and with expriment where data from these two sources are available. We assign an accuracy related to the reliabilitiy of the underlying data on which the expressions are based.

A significant effort has previously been devoted to this type of review and derivation of algebraic representations. Matsunami *et al* [1], provide a complete compendium of data through 1983 with algebraic fitting formulae similar to those we will use here; this supersedes their earlier report [2]. They have also provided an update on the fitting procedures [3]. There is also a compendium of data concerning angular distribution of ejected species produced by the same group [4]. Bohdansky [5] provides a valuable review of sputtering related to fusion that is largely based on the work of the group at IPP/Garching; the raw data points of that group for work published prior to 1979 can be found in the report by Roth *et al* [6]; an update of that review can be found in ref.

[7]. A further useful compendium of data covering both light and heavy projectiles is to be found in the work of Andersen and Bay [8]. While this document was in preparation, an update to references [6] and [7] was published by Eckstein, *et al* [9].

2. SCALING RELATIONS

Adapting from the work of Bohdansky [10] we write the expression for sputtering as follows:

$$Y(E_o) = Y^*(E_o)\, g(E_{th}/E_o) \qquad (1)$$

The term Y^* represents the general behaviour of sputtering in a high energy region where threshold effects are unimportant; we shall use for this an expression introduced by Sigmund [11]. The term $g(E_{th}/E_o)$ is a threshold function to describe the decrease of yield as one approaches the projectile threshold energy for sputtering, E_{th}; there is no reliable theoretical form for this expression and it is generally established by comparison with experiment. We shall examine each of these terms in detail to suggest algebraic forms and point out parameters that can only be evaluated by reference to subsidiary information or by direct fitting to experimental data. Finally we shall return to a full restatement of Eq. (1) that may be used for predictive purposes.

2.1. Generalized Sputtering Yield, Y^*

Again from the work of Bohdansky [10] we write the generalized relation for sputtering derived from the work by Sigmund [11] as follows:

$$Y^*(E_o) = \frac{0.042}{U_o}\ \alpha\ S_n(E_o) \qquad (2)$$

where E_o is the impact energy of the projectile. U_o is the binding energy of surface atoms in the target; this is generally taken as the sublimation energy, and S_n is the nuclear stopping. The factor α is an energy independent parameter, which in the Bohdansky's formulation was a function of the ratio of projectile and target masses M_1 and M_2 respectively. It is then suggested that the nuclear stopping power may be represented by a universal function of a reduced energy parameter (ε) in the form where ε is a reduced energy

$$S_n(E_o) = 4\pi a\ Z_1 Z_2 e^2\ \frac{M_1}{M_1+M_2}\ s_n(\varepsilon) \tag{3}$$

$$\varepsilon = \varepsilon_L\ E_o \tag{4}$$

and ε_L is given by

$$\varepsilon_L = \frac{M_2}{M_1+M_2}\ \frac{a}{Z_1 Z_2 e^2} \tag{5}$$

and a is the screeing length for the potential

$$a = \frac{0.885\ a_o}{(Z_1^{2/3}+Z_2^{2/3})^{1/2}} \tag{6}$$

with a_o being the Bohr radius for hydrogen.

The factor s_n is a function of reduced energy ε only, so the expression for sputtering represents a universal function for all projectile target combinations. Again following the lead of Bohdansky [10] we will adopt the following form for $s_n(\varepsilon)$

$$s_n(\varepsilon) = \frac{C\ \varepsilon^{1/2} ln(\varepsilon+2.718)}{1+A_1\varepsilon^{1/2}+A_2\varepsilon+A_3\varepsilon^{3/2}} \tag{7}$$

The determination of the constants is discussed in Sec. 4.1.

2.2. The Threshold Function $g(E_{th}/E_o)$

The threshold function is a dimensionless factor that represents the modification of the generalized sputtering yield Y* to account for the finite energy required to remove a target atom from the surface; it must be zero at the threshold and become unity at some energy. There is no reliable analysis at present that seeks to derive the form of the function from theory. Based on analysis of a wide variety of experimental data Bohdansky [10] suggests the form

$$g(E_{th}/E_o) = \left[1 - \left[\frac{E_{th}}{E_o}\right]^{2/3}\right]\left[1 - \frac{E_{th}}{E_o}\right]^2 \quad (8)$$

This functional form has some basis in theory but is justified primarily from the analysis of experimental data.

The true value of the threshold energy must be related to the precise details of the collision processes and the surface condition. For the present consideration of light projectile ($M_2/M_1 > 1$) we follow Behrisch and Weissmann [12] and propose that the sputtering at threshold is due to projectiles reflected from some depth in the solid returning to the surface and engaging in a head on collision with a surface atom; if the energy transferred in this second collision exceeds the binding energy U_o then the target atom is ejected. On this basis the lowest projectile energy that will eject a surface atom, or the threshold energy, will be

$$E_{th} = \frac{U_o}{\gamma(1-\gamma)} \quad (9)$$

where

$$\gamma = \frac{4\,M_1M_2}{(M_1+M_2)^2} \quad (10)$$

is the energy transfer from projectile to a target atom in a head-on collision. As a justification for the choice of a two scattering event sequence we note that experimental studies of light ion backscattering from surfaces [13] demonstrate that the most energetic recoils to the surface have suffered only a single large-angle scattering event rather than multiple small-angle scattering.

2.3. The Total Yield Y

Combining equations (1-3) and (6-8) expressed in terms of reduced energy we arrive at

Ideally we regard Eq. (11) as representing the functional dependence of sputtering

$$Y(\varepsilon) = \frac{0.042}{U_o}\alpha\ 4\pi\ \frac{0.885\ a_o}{(Z_1^{2/3}+Z_2^{2/3})^{1/2}}\ Z_1 Z_1 e^2$$

$$x\ \frac{M_1}{M_1+M_2}\ \frac{C\,\varepsilon^{1/2}\ln(\varepsilon + 2.718)}{1+A_1\varepsilon^{1/2}+A_2\varepsilon+A_3\varepsilon^{3/2}}\left[1 - [\frac{\varepsilon_{th}}{\varepsilon}]^{2/3}\right]\left[1 - \frac{\varepsilon_{th}}{\varepsilon}\right]^2 \qquad (11)$$

yield on projectile energy and on the nature of the colliding species. We first seek to validate the general form of the equation; this would possibly require separate test of the threshold function of Eq. (8) which dominates at low energy and then test of the nuclear stopping term of Eq. (7) which dominates at high energy. We then need to establish the various unknown factors by comparison with experimental or other data. These unknown factors included the constants C, A_1, A_2, A_3, in Eq. (7) for nuclear stopping, which should be the same for all collision species, the value of the threshold energy E_{th} which will relate to the specific collision combination and the value of α whose precise form is unknown and which we assume will be different for each set of collision partners. It is unreasonable to fit Eq. (11) to the experimental data with all the unknown paramters as free variables to both validate the equation's form and to determine the relevant unknown factors. The quality of the experimental data is usually quite inadequate to support such a procedure. Rather we need to examine these matters by consolidating together information on each of these separate issues of validation and parameter determination.

We will first review briefly the nature and quality of available numerical data with which these various formulations may be compared and then return to the validation of Eq. (11) and the establishment of the unknown parameters.

3. AVAILABLE NUMERICAL DATA

In order to fit the above equations and establish the unknown parameters, one requires a data base that covers a broad range of collision cases and is of high statistical accuracy. Ideally we would use experimental information, but regrettably this is at present inadequate. Experiments are generally performed by measurements of weight loss resulting from sputtering. For light projectile impact weight losses are small and statistical uncertainties large. Corrections must be made for mass gain due to retention of projectiles in the target. The projectiles may combine chemically with the target (e.g. hydrogen ions in titanium) thereby changing the target composition. Since atom ejection occurs from the first one or two atomic layers, the influence of surface layers of oxides or other contaminants may be severe. For a case such as titanium sputtered by hydrogen there exists projectile retention and a high possibility of a contaminant oxide layer; under those circumstances one does not know whether the weight loss resulting from sputtering is due to removal of O, H or Ti. In genera,l experimental data is of poor statistical accuracy and often tells us little about the near- threshold region and may involve significant systematic errors. While experimental data may not be adequate for a detailed test of the equations, we must however insist that any fitted expression be consistent with experiment to within the accuracy of the data. For the present work we generally use experimental data quoted in the compendia of Matsunami et al. [1] with a preference for the extensive data sets produced by the Garching group; numerical values of the data from Garching may often be found in their own compendia [6,9].

The other type of information which is pertinent to the comparison are the Monte Carlo calculations by codes such as TRIM and MARLOWE. These codes are designed for the general description of collisional processes in solids and produce data not only for sputtering but for range, implantation profiles, and reflection. The results of these codes have been checked numerous times against various types of experimental data and they appear to be quite reliable. Both TRIM and MARLOWE are based on binary collision models and require adoption potentials and expressions for the energy loss. MARLOWE was designed for single crystals but can deal with amorphous targets by randomly

rotating the lattice cell between collision events. The TRIM code deals directly with amorphous targets and runs more rapidly. It has been shown [14] that these two codes give essentially the same results provided one adopts the same input information. An important parameter is the choice of the potential for the scattering process. In the original expressions of the codes a Moliere potential was chosen [14] but a recent analysis of different potentials [15] has led Eckstein [16] to adopt a Kr-C potential. Monte Carlo calculations generally have a statistical accuracy of 10%. The results may, however, be altered by as much as 30% by the choice of potentials and other relevant parameters. Many of the calculated data that we shall use here have been provided privately by Eckstein [17] and are now published in Ref. [9].

4. FITTING TO THE AVAILABLE DATA

The general form of Eq. (11) was proposed first by Bohdansky [5] who carried out fitting procedures and evaluated the various unknown factors by comparison with experiment and various other subsidiary data. We shall first review that previous work. Then we shall re-evaluate the constants of Eq. (11) by comparison first with the recent Monte Carlo simulations and then comparison with experiments.

4.1. The Bohdansky Approach

In Bohdansky's work [5,10] the form of the nuclear stopping expression, Eq. (7), and the magnitudes of the constants C, A_1, A_2, A_3 were taken from Matsunami et al. [18] who fitted Eqs. (3) and (7) to theoretical stopping power data by Lindhard et al. [19]. The values derived for the constants were

$$C = 3.441,\ A_1 = 6.35,\ A_2 = -1.708,\ A_3 = 6.882. \qquad (12)$$

Lindhard's stopping power predictions were for a general case, covering high mass projectiles and it is not at all clear that they should be applicable to the light projectile impact situations that are the focus of this report. They have never been validated against experimental data.

The functional form of the threshold behaviour in Eq. (8) was validated [10] by comparison with a large body of experimental data including both light and heavy particle sputtering. Within the validation the value of threshold energy was established by fitting to the experimental data. The functional dependence on energy is quite adequate. We should note however that Matsunami et al. [1] obtained equally good fits with a slightly different form of threshold function. The values of energy threshold and of the factor α were determined simultaneously by the fit of Eq. (11) to experimental data. They are thus interdependent. The derived values of energy threshold did not follow a predictable variation with binding energy and particle masses; specifically Eq. (9) did not represent the threshold energies determined by fitting. We will recall that experimental data close

to threshold are not expected to be of high reliability. With uncertainty in the energy threshold, it is not clear what is the reliability of the parameter α determined during the same fitting procedure.

The constants in the nuclear stopping term, Eq. (7), were established by a fitting to a theory that is not necessarily applicable to the present case of light projectile impact and has never been tested against experimental data. We shall demonstrate shortly that the constants utilized are not consistent with TRIM simulations. The values of threshold energy derived from fitting to experiment do not relate in a systematic fashion to the surface binding energy. Perhaps this is due to the very high uncertainty of near-threshold experimental data points. Since experimental data points often exhibit scatter over factors of two and three it is not clear whether the comparison of Eq. (11) with experiment provides a satisfactory validation.

While the Bohdansky fittings were adequate to represent the data available at that time, there remains a high degree of uncertainty in the results which provides substantial reason to re-examine the details of the fitting procedures.

Eckstein *et al* [9], using a revised Bohdansky formula, fit both experimental and simulation data. The revised formula was obtained by replacing the Thomas-Fermi potential by the Kr-C potential, potential used in the Monte Carlo codes, in the nuclear stopping cross section.

4.2. Present Approach

Bohdansky's tests relied in part on poor quality experimental measurements of sputtering and in part on untested generalized theoretical predictions of nuclear stopping. We propose to validate and test the form of Eq. (11) against TRIM simulations of sputtering and then confirm the validation against experiment. As test data we utilize a group of TRIM simulations supplied by Eckstein [9,17] that we reproduce for reference in Fig. 1. The data appear to have a high degree of statistical reliability and extend over a large energy range. An important feature of the procedure is that we develop a reduced sputtering yield formulation that allows us to utilize the whole group of data for a single test of our formulations; this helps remove statistical fluctuations and minimize

the influence of errors confined to individual cases.

As a first step Eq. (11) is rearranged to give a reduced sputtering yield $G(\varepsilon)$ as a function of the reduced energy ε

$$G(\varepsilon) = Y(\varepsilon) \frac{(Z_1^{2/3}+Z_2^{2/3})^{1/2}}{Z_1 Z_2} \frac{(M_1+M_2)}{M_1} U_o \left[1 - \left[\frac{\varepsilon_{th}}{\varepsilon}\right]^{2/3}\right]^{-1} \left[1 - \frac{\varepsilon_{th}}{\varepsilon}\right]^{-2}$$

$$= 3.558\, \alpha\, s_n(\varepsilon) \qquad (13)$$

Aside from the factor α, the reduced sputtering yield expression is independent of projectile-target combination and it should be possible to express all the TRIM data with a single curve.

Fig. 1 shows the sputtering yield as a function of projectile energy (keV) from Monte Carlo calculations by the TRIM code [9,17]. The meaning of the lines is explained below. The TRIM data of Fig. 1 have been converted into reduced sputtering yield by Eq. (13) and replotted in Fig. 2. Threshold energies were calculated from Eq. (9), that is based on ejection by recoiling projectiles. The data for H^+ impact on Ni and for D^+ and He^+ impact on Ti are shown as calculated; the data for D^+ and He^+ on Ni and for He^+ impact on Fe have been normalized slightly (0.78, 0.86 and 0.74 respectively) to lie on the same general curve; such a shift merely indicated that α is not the same for each collision combination and that is not unexpected.

Fig. 2 demonstrates that the reduced sputtering yield $G(\varepsilon)$ has single functional dependence on energy for a wide range of collision combinations. This validates the general form of Eq. (1) on which this analysis is based. In establishing the reduced sputtering yield we have factored out the threshold behaviour using the proposed function of Bohdansky shown in Eq. (8) and the notion of threshold energy being related to ejection by reflected projectiles given in Eq. (9). Agreement of these data sets at the lower energies validates the use of these two equations to represent TRIM simulations of sputtering.

We have fitted the nuclear stopping term of Eq. (7), proportional to the reduced

sputtering $G(\varepsilon)$, to the composite of data in Fig. 2 and determine appropriate values of the constants. We have normalized our fit at high energies to Bohdansky's nuclear stopping equation by putting the following constraint on the fitting parameters: $A_3/C = 2$ The following values for the parameters were obtained:

$$A_1 = 2.0596,\ A_2 = 1.5667,\ A_3 = 8.3248,\ C = 4.1624 \tag{14}$$

These are different from the values in Eq. (12) used by Bohdansky [10], which were derived from theoretical predictions of heavy particle nuclear stopping. We also show in Fig. 2 Bohdansky's plot of s_n. Clearly the equation used by Bohdansky does not represent the TRIM data at energies below 2 keV.

Combining Eqs. (11) and (114) we arrive at the following expression for Y (E_o):

$$Y(E_o) = \frac{14.81\alpha}{U_o} \frac{Z_1 Z_2}{(Z_1^{2/3}+Z_2^{2/3})^{1/2}} \frac{M_1}{M_1+M_2} \frac{\epsilon^{1/2} \ln(\epsilon+2.718)}{3+2.0596\epsilon^{1/2}+1.5667\epsilon+8.3248\epsilon^{3/2}}$$

$$x\left[1 - (\frac{E_{th}}{E})^{2/3}\right]\left[1 - \frac{E_{th}}{E}\right]^2 , \tag{15}$$

where E_o and U_o are in eV and the reduced energy is given by

$$\epsilon = 3.255\ x\ 10^{-2} \frac{M_2}{M_1+M_2} \frac{E_0}{Z_1 Z_1 (Z_1^{2/3}+Z_2^{2/3})^{1/2}} . \tag{16}$$

The parameter α is given in Table 2 for the different cases studied here along with M_1, M_2, Z_1, Z_2 and U_o

The lines in Fig. 1 were obtained by fitting the TRIM results with Eq. (7) using the parameters in Eq. (14). The corresponding values of α are given in Table 1. We may conclude that Eq. (11), with the threshold energy predicted in terms of ejection by recoiling projectiles and with the constants given in Eq. (14), represents well a group of TRIM simulation data. The sole unknown factor is α, which from the original expression of the formulation is expected to be only a function of projectile and target masses. α appears as a multiplicative constant establishing the magnitude of the sputtering yield

function.

The validation of Eq. (11) has so far been in terms of TRIM simulations. We must now review whether Eq. (11) is as successful in representing experimental data. We further need to establish α for individual collision cases which we also prefer to do by comparison with experiment.

4.3. Evaluation of α and Test Against Experimental Information

We now test the proposed formula, Eq. (11), against experimental information and evaluate the remaining unknown factor α for each specific projectile-target collision case. It is our preference to evaluate α from experiment. Since α occurs as a simple multiplicative constant, a fit to a set of data points will use the complete set with equal weighting, which in part compensates for the limited statistical accuracy of individual experimental points.

We have fitted Eq. (11) to experimental data for all projectile target combinations of interest; the single unknown parameter to be derived from the fit is α. The values obtained are listed in Table 1. Agreement with experiment is within the estimated experimental uncertainties for most cases. The major areas of discrepancy occur when the measured sputtering yield may involve a component due to chemical sputtering (e.g. H and D sputtering of carbon), where the target may chemically combine with the projectile (e.g. H and D sputtering of Ti) and where the target may be expected to have a significant oxide layer (e.g. Ti).

In Fig. 3 we show data for sputtering of Ni by H^+, D^+, and He^+ as a function of the projectile energy. There are both experimental as well as TRIM simulation data for each case and these are in good agreement. We should note that the experimental data shows considerable statistical fluctuation. There are significant discrepancies between simulation and experiment only at the lowest energies where the experiments are likely to be most difficult; this is particularly obvious for the H^+ + Ni data at energies less than 0.1 keV. The fitted lines for H^+ and D^+ are essentially the same for experiment and theory; only for He^+ there is some difference corresponding to about 20% in the absolute magnitudes. We conclude in these cases that Eq. (11) is an excellent representation of

both the simulation and experiment. We choose the factor α from the fit to the experimental data.

In Fig. 4 we show a similar plot of the data for sputtering of Mo. In this case there is simulation data for the case of He^+ and D^+ impact, [9,17]. We observe that while the simulation data for He^+ is in agreement with experiment the one for D^+ is in disagreement by more than a factor of two. Again there are considerable discrepancies between experimental data points. In this case we choose the experimental data as a basis of the fit to arrive at α.

In Fig. 5 we show the corresponding plots for sputtering of a Ti target. This is a very difficult case. The Ti undoubtedly carries a contaminant oxide layer that will influence yield measurements. This layer is likely to vary with the nature of the experimental conditions (beam flux, residual gas pressure, prior history etc). Also we anticipate that for H^+ and D^+ impact the projectiles will chemically bond with the target so changing chemical composition systematically with bombardment dose and significantly changing the binding energy. As evidence of the experimental problems we point to the data for the repetitive measurement of yield for He^+ on Ti at an energy of 3 keV. The experimental data points spread over more than one full order of magnitude The problems of contamination and projectile retention will influence the binding energy appropriate to the sputtering process and this influences not only absolute magnitude but also the assessment of an appropriate energy threshold. Also, of course, in these weight loss experiments it is not clear what the weight loss corresponds to; it will represent a combination of losses of Ti, O and H (or D). It is not al all suprising that neither the TRIM data nor the form of Eq. (11) agree with experiment either in magnitude or in functional dependence on projectile energy. In this case we still use Eq. (11) to represent sputtering yield and still evaluate the parameter α from experimental data. However, we assign a very low limit of reliability to the fitting parameters.

Fig. 6 shows the corresponding plots for Be. The experimental points are either scarce, as in H^+ and He^+, or spread over more than an order of magnitude. The TRIM results are in disagreement with both experiment and the present fit. The Be case is the

worst of all the cases studied. Still we arrived at a value of α, but give it a very high percentage uncertainty (100%). Fig. 7 shows the plots corresponding to B. In these cases there are very few experimental points and they are only over a small region of energy. Again we obtained a value for α and give it a very high percentage uncertainty (100%). Fig. 8 corresponds to C. As in the case of Ti, there are considerable experimental difficulties, especially at low energies. There are large discrepancies between the available simulation and experimental data, especially at low energies. We assign an uncertainty of 50%. Fig. 9 corresponds to Al. As in C and Ti, experimental difficulties result in erratic statistical fluctuations among quoted experimental data, especially for H^+. The simulation data available agrees well with experiment and with the present fit and therefore, we assign 30% uncertainty. Fig. 10 shows the corresponding plots for Fe. The agreement between the present fits and experiment is within experimental accuracy for H^+ and D^+ at all energies, while for He^+ the low energy region data are in disagreement. The simulation data for He, agrees well with the fit, even though α was obtained from the experimental points. We assign an uncertainty of 20-30%.

Figs. 11-13 show the corresponding plots for Cu, W and Au. In these cases both the fits and the available simulation data are within experimental accuracy. The accuracy assigned to α is therefore better. The uncertainty assigned is 20%.

In Table 2 we have summarized the derived information on the mass dependent factor α. A brief comment indicates our assessment of reliability of the fit.

5. SYSTEMATIC BEHAVIOR OF α

Following Bohdansky [10] we have plotted in Fig. 14 the values of α as a function of mass ratio M_2/M_1 for the various targets considered here. Also shown is Bohdansky's calculation of α as a function of mass ratio that is applicable only to low mass ratio cases. The general form of the present data is similar to that published earlier by Bohdansky [10]. There are however differences in magnitudes due to our use of a different set of constants in the formulation of s_n. From Fig. 14 it is quite clear that, for these light projectile sputtering cases, there is no single dependence of α on mass ratio. Rather the behaviour of α is a function of the nature of the target.

One would hope to be able to use the data of Fig. 14 to interpolate for cases that have not yet been the subject of experimental test. One particular situation of general importance is the value of α for T^+ sputtering; a case which has never been experimentally tested for any target. In view of the monotonic variation of α with mass ratio for each target one might reasonably estimate the value of α for T^+ impact as lying midway between the values for D^+ and He^+ impact. This, coupled with the use of Eq. (12), should give an estimate of sputtering yield that is as reliable as the measurements for H^+, D^+, and He^+.

Even though the behavior illustrated in Fig. 14 does not provide a systematic picture that would allow us to make an estimate of yield for a target that has not previously been studied, we have interpolated α for the cases T^+ + Mo and T^+ + W, cases for which there are recently published simulation data [9]. The values of α obtained are 0.175 and 0.21 for Mo and W respectively. Fig. 15 shows the sputtering yield of Mo. The dotted line is the T^+ case, using the interpolated α, and the diamonds are the simulation results. Notice that the disagreement between the simulation data and the present fit for T^+ and D^+ is similar, suggesting that the discrepancy is due mainly to the fact that α was obtained from experimental data, and there are significant discrepancies between simulation and experiment. A similar case is shown in Fig. 16 for the sputtering yield of W.

6. CONCLUSION

We have presented a general expression for sputtering yield that has been validated by comparison with TRIM simulations. Comparison with experimental data was made when data was available. This equation (Eq. 11) with suitable constants can be used to predict the sputtering yield as a function of energy and will agree with both experiment and simulation to within the accuracy of these data sources.

The semi-empirical formula introduced by Bohdansky [10] to represent experimental observations of threshold behaviour is found also to satisfactorily represent TRIM simulations. The use of a threshold energy related to ejection by recoiling projectiles is found to be consistent with the simulations. After correcting the TRIM simulations for threshold effects and expressing all data in terms of a reduced energy the results for a wide variety of collision partner combinations exhibit the same functional dependence on reduced energy. According to the original formulation of our equations, that form should be related to nuclear stopping power. We find however that the constants required in our formula are different from those derived by fitting directly to nuclear stopping predictions. This is perhaps not surprising since the nuclear stopping prediction was designed for heavy projectiles, while we are here concerned with light projectiles where the collision cascades are likely to be different. Our formula for s_n, with the constants derived from comparison with TRIM, Eq. (14), should be considered as a representation of sputtering behaviour and is not necessarily an indication of nuclear stopping.

There remains in the formulation the factor α which was originally introduced to represent the fraction of the near-surface collision cascade energy that results in ejection; it is supposed to be dependent only on the target/projectile mass ratio. We treat this as an unknown parameter that must be found by fitting to individual data sets. The values determined are in fact related not only to mass ratio but also to the type of target species. There is no apparent rule governing the behaviour of α for different collision situations. This is not surprising since α was introduced originally in a formulation to represent sputtering for high mass ratio situations where ejection occurs primarily as a result of

multiple collisions in the collision cascade. For light projectiles it seems likely that an additional ejection mechanism is due to recoiling projectiles colliding with surface atoms. The relevence of α for light ion sputtering is unclear and we retain it as a fitting factor that must be established empirically for each case of interest.

Eq. (11) may be used to represent experimental and TRIM simulation data for light projectile sputtering of candidate plasma-facing fusion reactor component materials. The equation should be used with the constants shown in Eq. (14) and with the threshold energy calculated by Eq. (9). The value of α for each case must be taken from Table 2 which is derived from fitting to experimental data. For the case of T^+ projectiles α may be estimated by mass-interpolation between the data for D^+ and He^+.

7. ACKNOWLEDGMENTS

We thank Drs. W. Eckstein and R.A. Langley for their critical reading of the manuscript and their useful comments.

REFERENCES

[1] N. Matsunami, Y. Yamamura, Y. Itikawa, N. Itoh, Y. Kazumata, S. Miyagawa, K. Morita, R. Shimizu and H. Tawara, "Energy Dependence of the Yields of Ion-Induced Sputtering of Monoatomic Solids", Institute of Plasma Physics, Nagoya, Report IPPJ-AM-32, 1983.

[2] N. Matsunami, Y. Yamamura, Y. Itikawa, N. Itoh, Y. Kazumata, S. Miyagawa, K. Morita and R. Shimizu, "Energy Dependence of Sputtering Yields of Monoatomic Solids", Institute of Plasma Physics, Nagoya, Report IPPJ-AM-14, 1980.

[3] N. Matsunami, Y. Yamamura, N. Itoh, H. Tawara and T. Kawamura, "Energy Dependence of Ion Induced Sputtering Yields of Monoatomic Solids in the Low Energy Region", Institute of Plasma Physics, Nagoya, Report IPPJ-AM-52, 1987.

[4] Y. Yamamura, Y. Itikawa and N. Itoh, "Angular Dependence of Sputtering Yields of Monoatomic Solids", Rep. IPPJ-AM-26, Institute of Plasma Physics, Nagoya University (1983).

[5] J. Bohdansky, Nuclear Fusion Special Issue 1984, p. 61 (1984).

[6] J. Roth, J. Bohdansky and W. Ottenberger, "Data on Low Energy Light Ion Sputtering", Max-Planck-Institut für Plasmaphysik, Garching, Report IPP 9/26, 1979.

[7] W. Eckstein, J. Bohdansky and J. Roth, Nuclear Fusion Supplement **1**, 51 (1991).

[8] H.H. Andersen and H.L. Bay, "Sputtering Yield Measurements", in Topics in Applied Physics, Volume 47, "Sputtering by Particle Bombardment I", R Behrisch, Ed., Springer-Verlag, Berlin, p. 145, 1981.

[9] W. Eckstein, G. Garcia-Rosoles, J. Roth and W. Ottenberger, " Sputtering Data", Max- Planck-Institut für Plasmaphysik, Garching, Report IPP9/82, 1993.

[10] J. Bohdansky, Nucl. Instrum. Meth. in Phys. Res. **B2**, 587 (1984).

[11] P. Sigmund, Phys. Rev. **184**, 383 (1969).

[12] R. Behrisch and R. Weissmann, Phys. Lett. **30A**, 506 (1970).

[13] R. Aratari and W. Eckstein, J. Nucl. Mater. **162-164**, 910 (1989).

[14] W. Eckstein, H. Verbeek and J.P. Biersack, J. Appl. Phys. **51**, 1194 (1980).

[15] D.J. O'Connor, J.P. Biersack, Nucl. Instrum. Meth. in Physics Research **B15**, 14 (1989).

[16] W. Eckstein and J.B. Biersack, Z. Phys. B - Condensed Matter **63**, 109 (1986).

[17] W. Eckstein, Private Communication, 1990.

[18] N. Matsunami, Y. Yamamura, Y. Itikawa, N. Itoh, Y. Kazumata, S. Myagawa, K. Morita and R. Shimizu, Rad. Eff. Lett. **57**, 15 (1980).

[19] J. Lindhard, V. Nielsen and M. Scharff, K. Dan Vid. Selsk. Mat. Phys. Medd. **36**, No. 10 (1958).

[20] C. Kittel, "Introduction to Solid State Physics" (John Wiley, New York, 1976). p. 74.

Table 1. Values of α determined by fitting to the TRIM results of Fig. (1)

Projectile	Target	Z_1	Z_2	M_1	M_2	ε_L (keV^{-1})	U_o[b] (eV)	α	Source and Notes
He^+	Ti	2	22	4	47.9	0.2222	4.85	0.256	a
D^+	Ti	1	22	2	47.9	0.4774	4.85	0.273	a
He^+	Fe	2	26	4	55.85	0.1814	4.28	0.337	a
H^+	Ni	1	28	2	58.69	0.3575	4.44	0.301	a
D^+	Ni	1	28	2	58.69	0.3516	4.44	0.368	a
He^+	Ni	2	28	4	58.69	0.1655	4.44	0.327	a

a: Work of Roth *et al* as reproduced in Ref. 1, supplemented by Refs. 9 and 17

b: From Ref. [20]

Table 2. Values of α determined by fitting to experimental data

Projectile	Target	Z_1	Z_2	M_1	M_2	ε_L (keV^{-1})	U_o^g (eV)	α	Accuracy %	Source and Notes
H^+	Be	1	4	1	9.01	3.9	3.32	0.129	100	a
D^+	Be	1	4	2	9.01	3.545	3.32	0.203	100	a
T^+	Be	1	4	3	9.01	3.249	3.32			
He^+	Be	2	4	4	9.01	1.39	3.32	0.257	100	a
H^+	B	1	5	1	10.811	3.008	5.77	0.412	50	b
D^+	B	1	5	2	10.811	2.773	5.77			
T^+	B	1	5	3	10.811	2.572	5.77			
He^+	B	2	5	4	10.811	1.118	5.77	0.358	50	b
H^+	C	1	6	1	12.00	2.414	7.37	0.303	50	c,d
D^+	C	1	6	2	12.00	2.242	7.37	0.391	50	c,d
T^+	C	1	6	3	12.00	2.092	7.37			
He^+	C	2	6	4	12.00	0.92	7.37	0.429	50	c
H^+	Al	1	13	1	26.98	0.9449	3.39	0.121	50	c
D^+	Al	1	13	2	26.98	0.9123	3.39	0.186	50	c
T^+	Al	1	13	3	26.98	0.8819	3.39			
He^+	Al	2	13	4	26.98	0.4087	3.39	0.253	50	c
H^+	Ti	1	22	1	47.9	0.4871	4.85	0.103	30	c,e
D^+	Ti	1	22	2	47.9	0.4774	4.85	0.121	30	c,e
T^+	Ti	1	22	3	47.9	0.4680	4.85			
He^+	Ti	2	22	4	47.9	0.2222	4.85	0.146	30	c,e
H^+	Fe	1	26	1	55.85	0.3934	4.28	0.275	30	c,e
D^+	Fe	1	26	2	55.85	0.3866	4.28	0.318	30	c,e

Projectile	Target	Z_1	Z_2	M_1	M_2	ε_L (keV^{-1})	U_o^0 (eV)	α	Accuracy %	Source and Notes
T^+	Fe	1	26	3	55.85	0.38	4.28			
He^+	Fe	2	26	4	55.85	0.1814	4.28	0.305	20	c,e
H^+	Ni	1	28	1	58.69	0.3575	4.44	0.308	20	c,e
D^+	Ni	1	28	2	58.69	0.3516	4.44	0.383	20	c,e
T^+	Ni	1	28	3	58.69	0.3459	4.44			
He^+	Ni	2	28	4	58.69	0.1655	4.44	0.367	20	c,e
H^+	Cu	1	29	1	65.34	0.342	3.49	0.500	20	c,e
D^+	Cu	1	29	2	65.34	0.3368	3.49	0.586	20	c,e
T^+	Cu	1	29	3	65.34	0.3317	3.49			
He^+	Cu	2	29	4	65.34	0.159	3.49	0.524	20	c,e
H^+	Mo	1	42	1	95.95	0.2121	6.82	0.083	20	c,e
D^+	Mo	1	42	2	95.95	0.2099	6.82	0.139	20	c,e
T^+	Mo	1	42	3	95.95	0.2087	6.82			
He^+	Mo	2	42	4	95.95	0.1006	6.82	0.185	20	c,e
H^+	W	1	74	1	183.92	0.1014	8.9	0.133	20	c,e
D^+	W	1	74	2	183.92	0.1008	8.9	0.185	20	c,e
T^+	W	1	74	3	183.92	0.1003	8.9			
He^+	W	2	74	4	183.92	0.0491	8.9	0.233	20	c,e
H^+	Au	1	79	1	197.00	0.09305	3.81	0.343	20	c,e
D^+	Au	1	79	2	197.00	0.09258	3.81	0.497	20	c,e
T^+	Au	1	79	3	197.00	0.09212	3.81			
He^+	Au	2	79	4	197.00	0.04515	3.81	0.486	20	c,e

Notes:

(a) Work of Roth et al. as reproduced in Ref. 8.
(b) Work of Migagawa et al. as reproduced in Ref. 1.
(c) Work of Roth *et al.* as reproduced in Ref. 1.
(d) Sputtering of carbon by hydrogen will include a component of chemical erosion not covered by our formulations. As a result the fitting procedure may be quite misleading.
(e) Supplemented by unpublished data. Refs. 9 and 17.
(f) Fits based on a small number of data points that are inadequate to validate proposed equations.
(g) From Ref. [20].

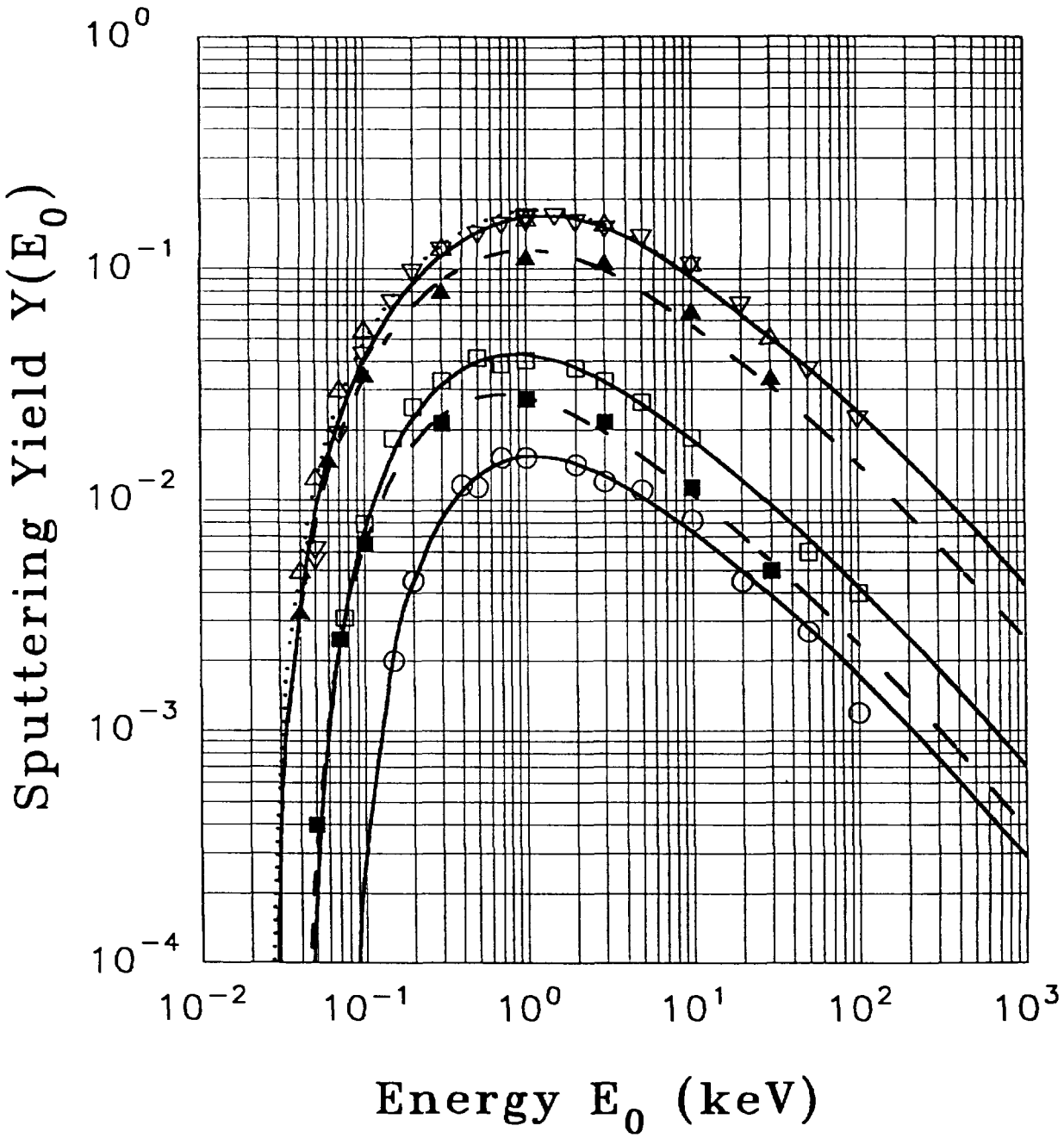

Fig. 1. Sputtering yield as a function of projectile energy (keV) calculated from Monte Carlo calculations by the TRIM code [9,17]. H^+ + Ni (open circles); D^+ + Ni (open squares); He^+ + Ni (open down triangles); He^+ + Fe (open up triangles); D^+ + Ti (full squares); He^+ + Ti (full triangles). The lines are the result of fits using equations (7) and (14), with the values of α given in Table 1.

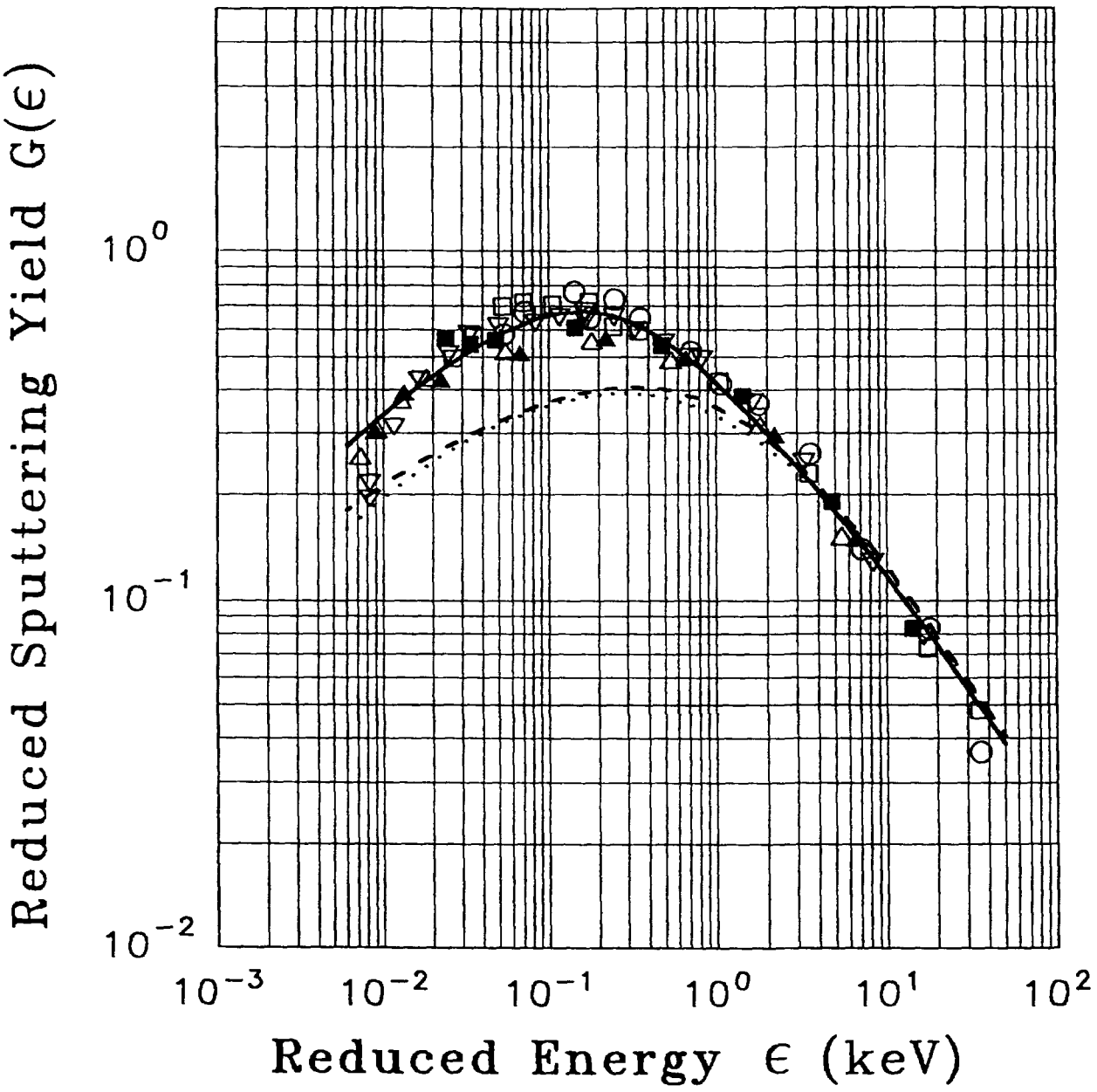

Fig. 2. Reduced sputtering yield $G(\varepsilon)$ defined by Eq. (13) plotted for the yield information shown in Fig. 1. The data points for D^+ and He^+ impact on Ti and for H^+ impact on Ni are shown as calculated. The data points for D^+, He^+ on Ni and for He^+ on Fe have been normalized to the other data at $\varepsilon=1$ to provide a composite curve. The solid line is the fit of Eq. (7) to the composite data; the resulting coefficients are shown in Eq. (14). For comparison we show Bohdansky's result of stopping power [5] (dashed line) and the result from the revised Bohdansky formula of ref. [9] (dotted line). The three curves coincide at large energies (see text). Data symbols as in Fig. 1.

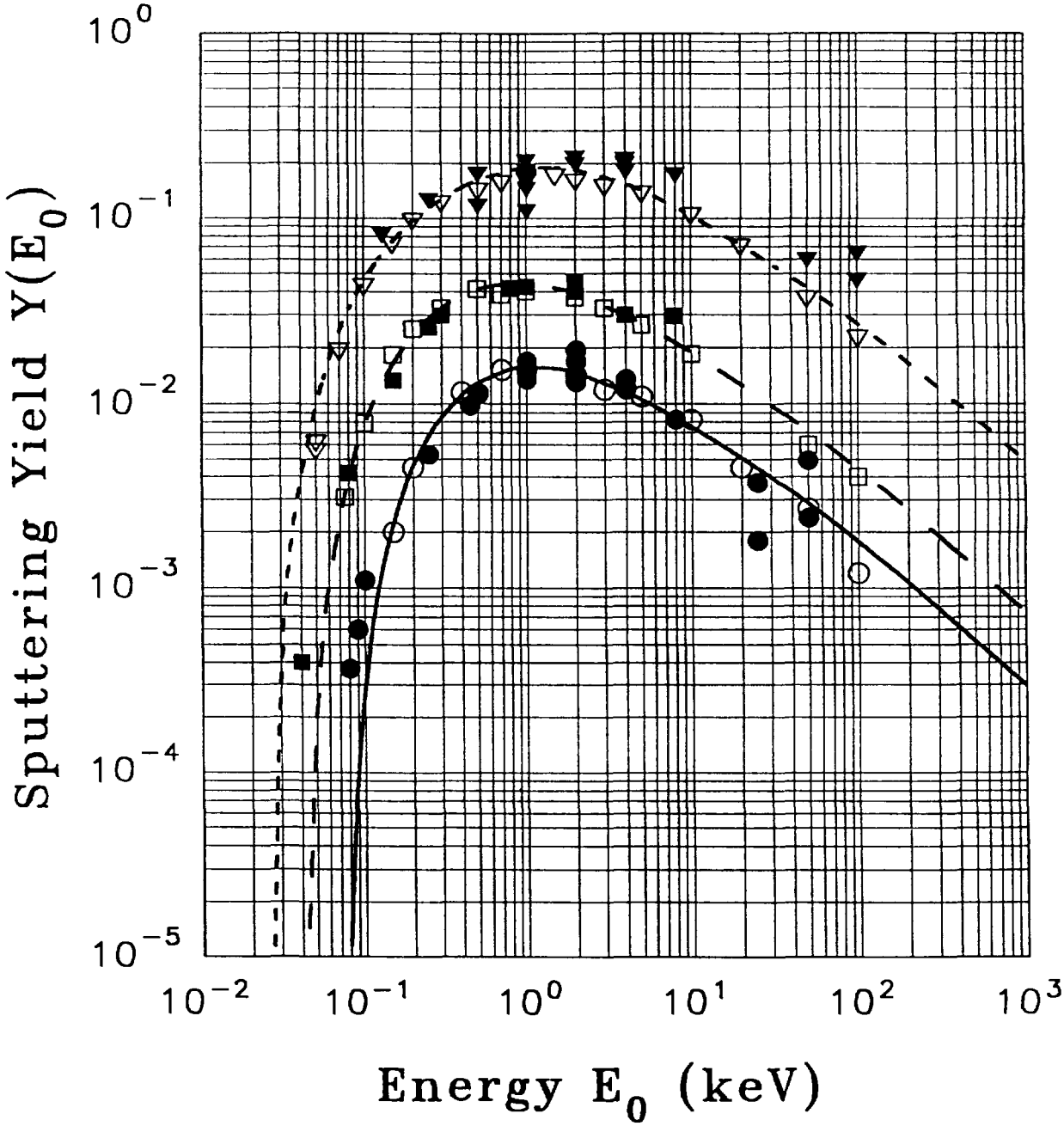

Fig. 3. Sputtering yield of Ni for impact of He^+ (triangles, short dashed line), D^+ (squares, dashed line) and H^+ (circles, full line) as a function of energy in keV. Full symbols are experimental measurements from the work of the Garching group taken from the report by Matsunami *et al* [1] with supplementary information from Refs. [9] and [17]. The open symbols are TRIM simulation results from Refs. [9] and [17]. Lines are the results of the present fit of Eq. 11 with the values of α shown in Table 2.

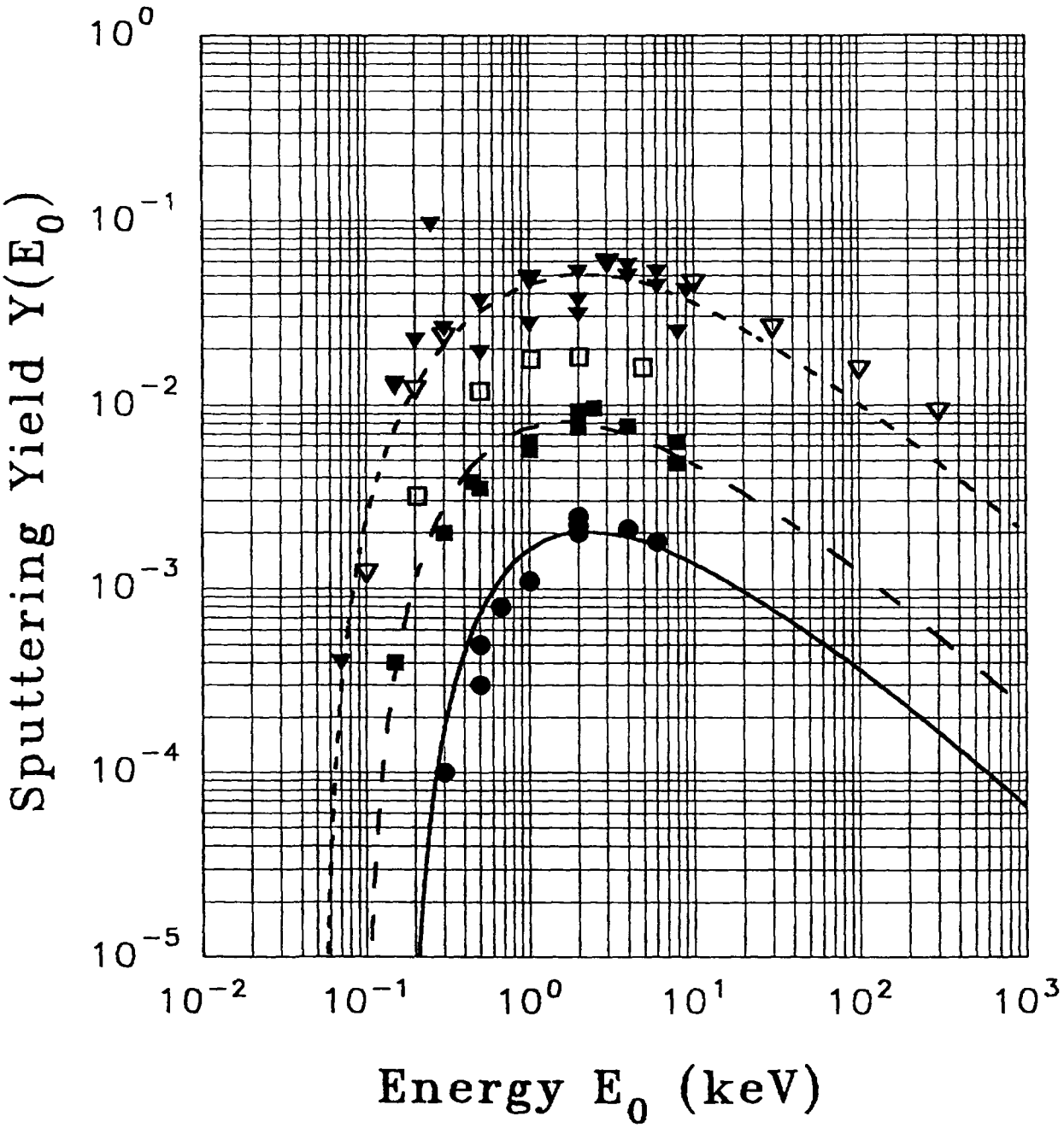

Fig. 4. Sputtering yield of Mo for impact of He^+ (triangles, short dashed line), D^+ (squares, dashed line) and H^+ (circles, full line) as a function of energy in keV. Full symbols are experimental measurements from the work of the Garching group taken from the report by Matsunami at al [1] with supplementary information from Refs. [9] and [17]. The open symbols are TRIM simulation results from Refs. [9] and [17]. Lines are the results of the present fit of Eq. 11 with the values of α shown in Table 2.

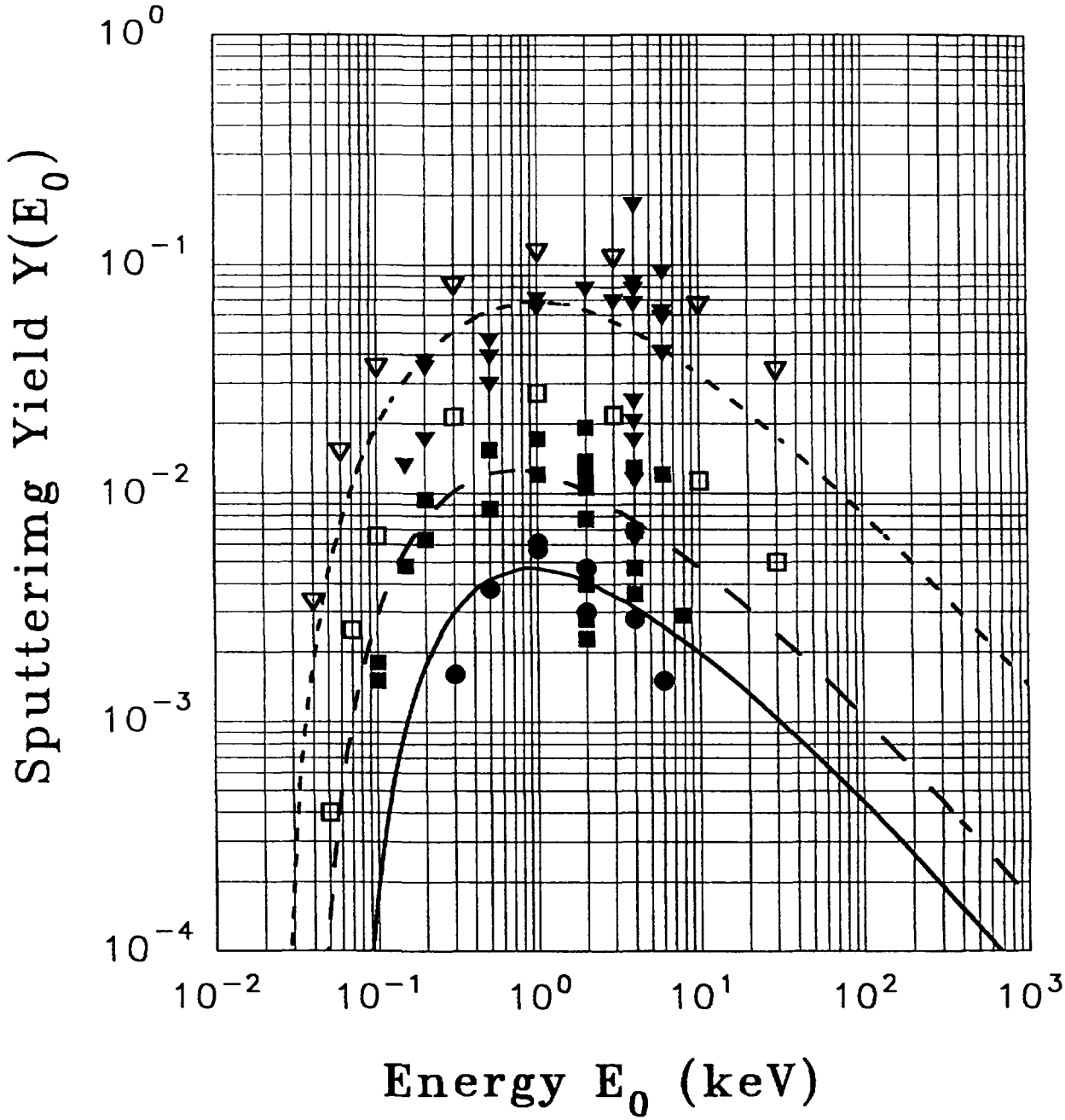

Fig. 5. Sputtering yield of Ti for impact of He^+ (triangles, short dashed line), D^+ (squares, dashed line) and H^+ (circles, full line) as a function of energy in keV. Full symbols are experimental measurements from the work of the Garching group taken from the report by Matsunami et al [1] with supplementary information from Refs. [9] and [17]. The open symbols are TRIM simulation results from Refs. [9] and [17]. Lines are the results of the present fit of Eq. 11 with the values of α shown in Table 2.

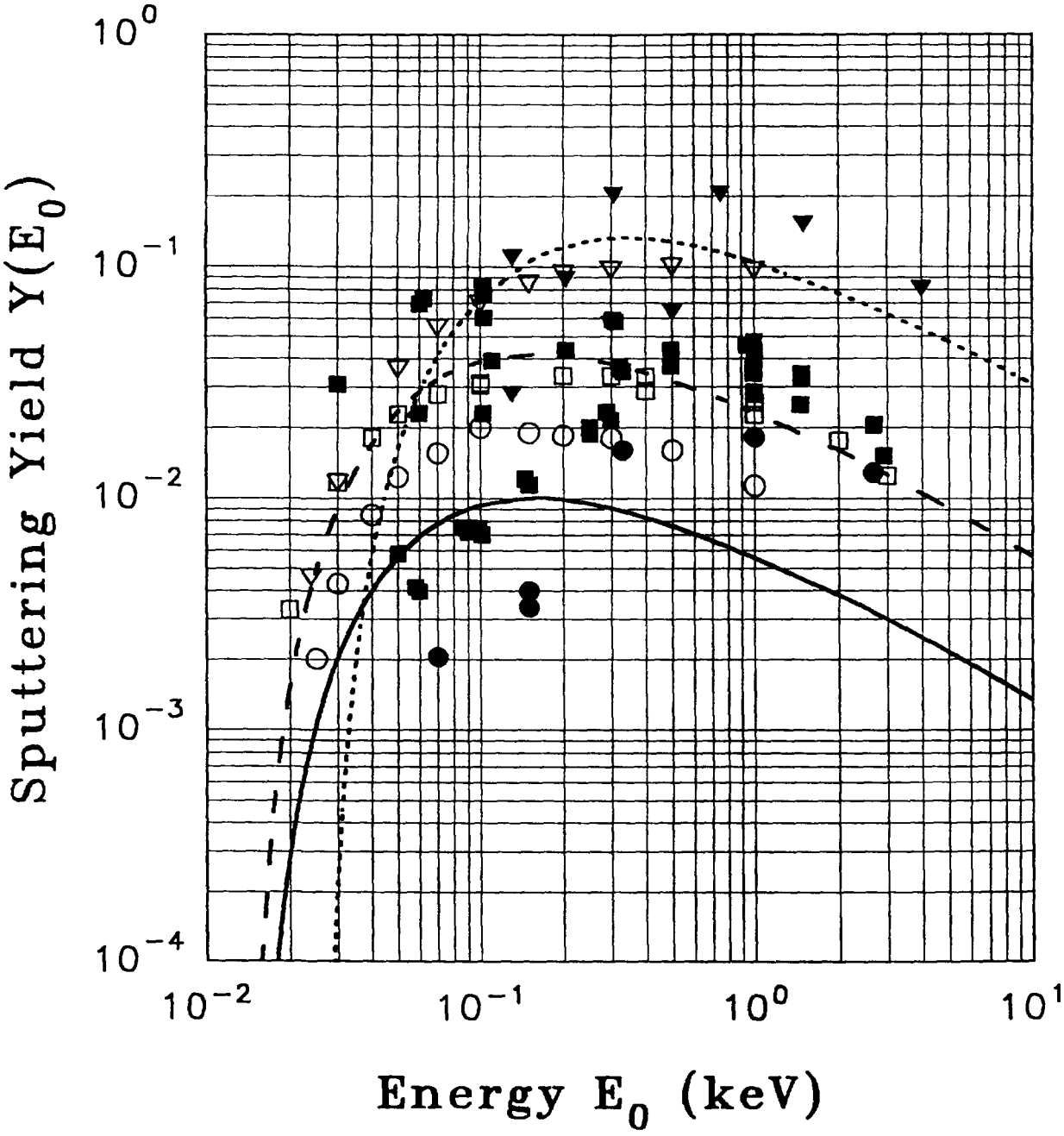

Fig. 6. Sputtering yield of Be for impact of He^+ (triangles, short dashed line), D^+ (squares, dashed line) and H^+ (circles, full line) as a function of energy in keV. Full symbols are experimental measurements from the work of the Garching group taken from the report by Matsunami et al [1] with supplementary information from Refs. [9] and [17]. The open symbols are TRIM simulation results from Refs. [9] and [17]. Lines are the results of the present fit of Eq. 11 with the values of α shown in Table 2.

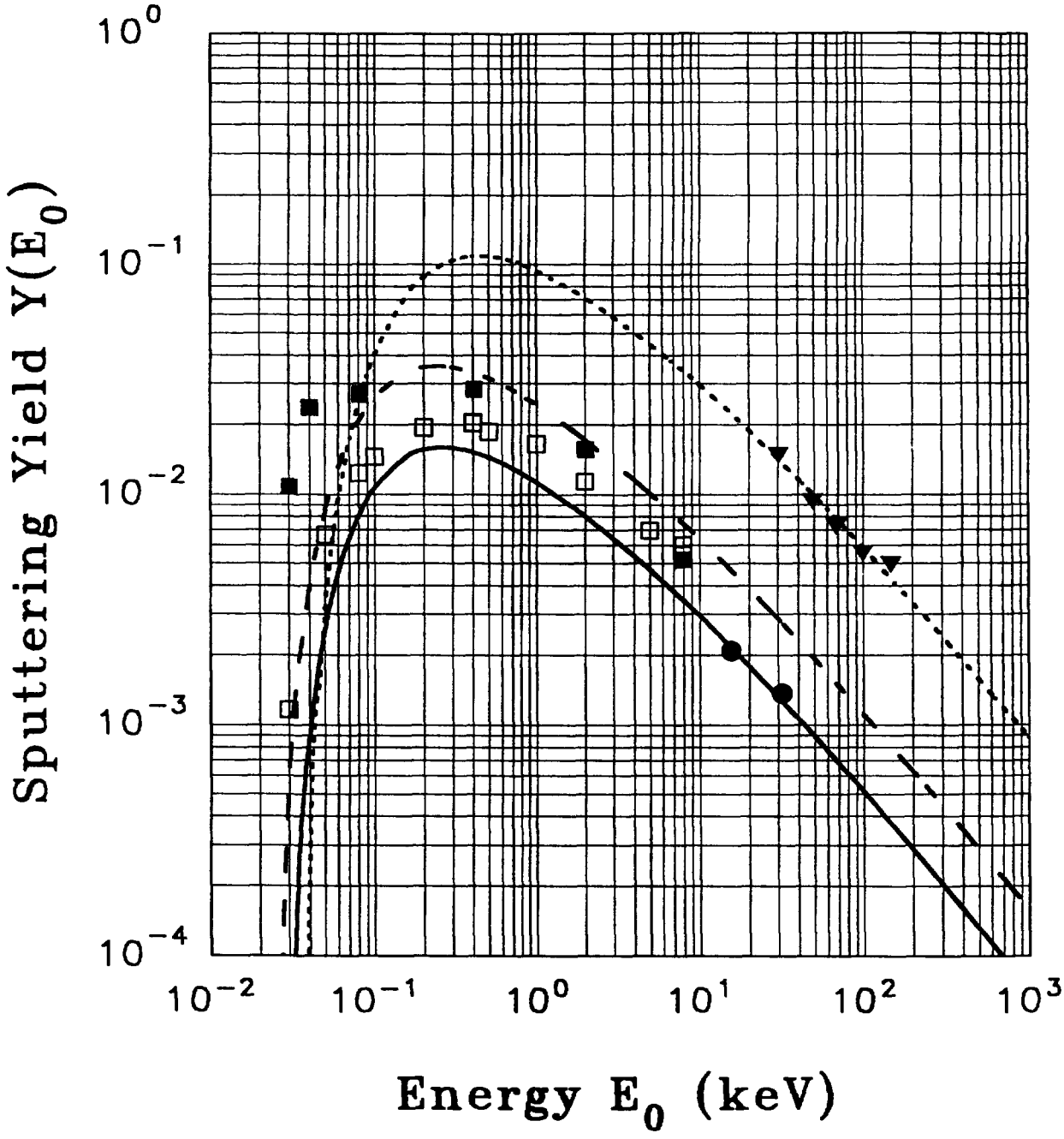

Fig. 7. Sputtering yield of B for impact of He^+ (triangles, short dashed line), D^+ (squares, dashed line) and H^+ (circles, full line) as a function of energy in keV. Full symbols are experimental measurements from the work of the Garching group taken from the report by Matsunami et al [1] with supplementary information from Refs. [9] and [17]. The open symbols are TRIM simulation results from Refs. [9] and [17]. Lines are the results of the present fit of Eq. 11 with the values of α shown in Table 2.

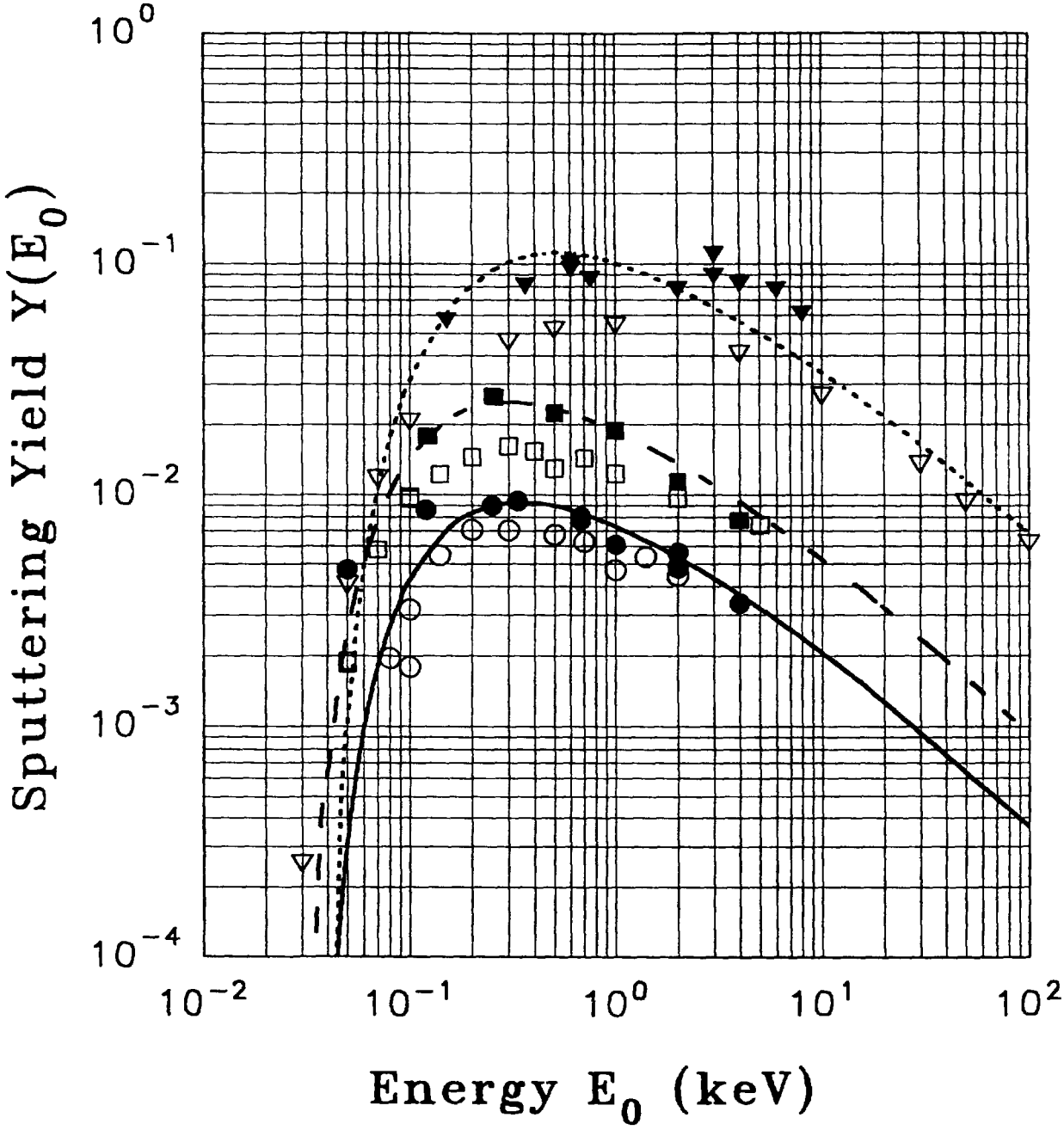

Fig. 8. Sputtering yield of C for impact of He^+ (triangles, short dashed line), D^+ (squares, dashed line) and H^+ (circles, full line) as a function of energy in keV. Full symbols are experimental measurements from the work of the Garching group taken from the report by Matsunami et al [1] with supplementary information from Refs. [9] and [17]. The open symbols are TRIM simulation results from Refs. [9] and [17]. Lines are the results of the present fit of Eq. 11 with the values of α shown in Table 2.

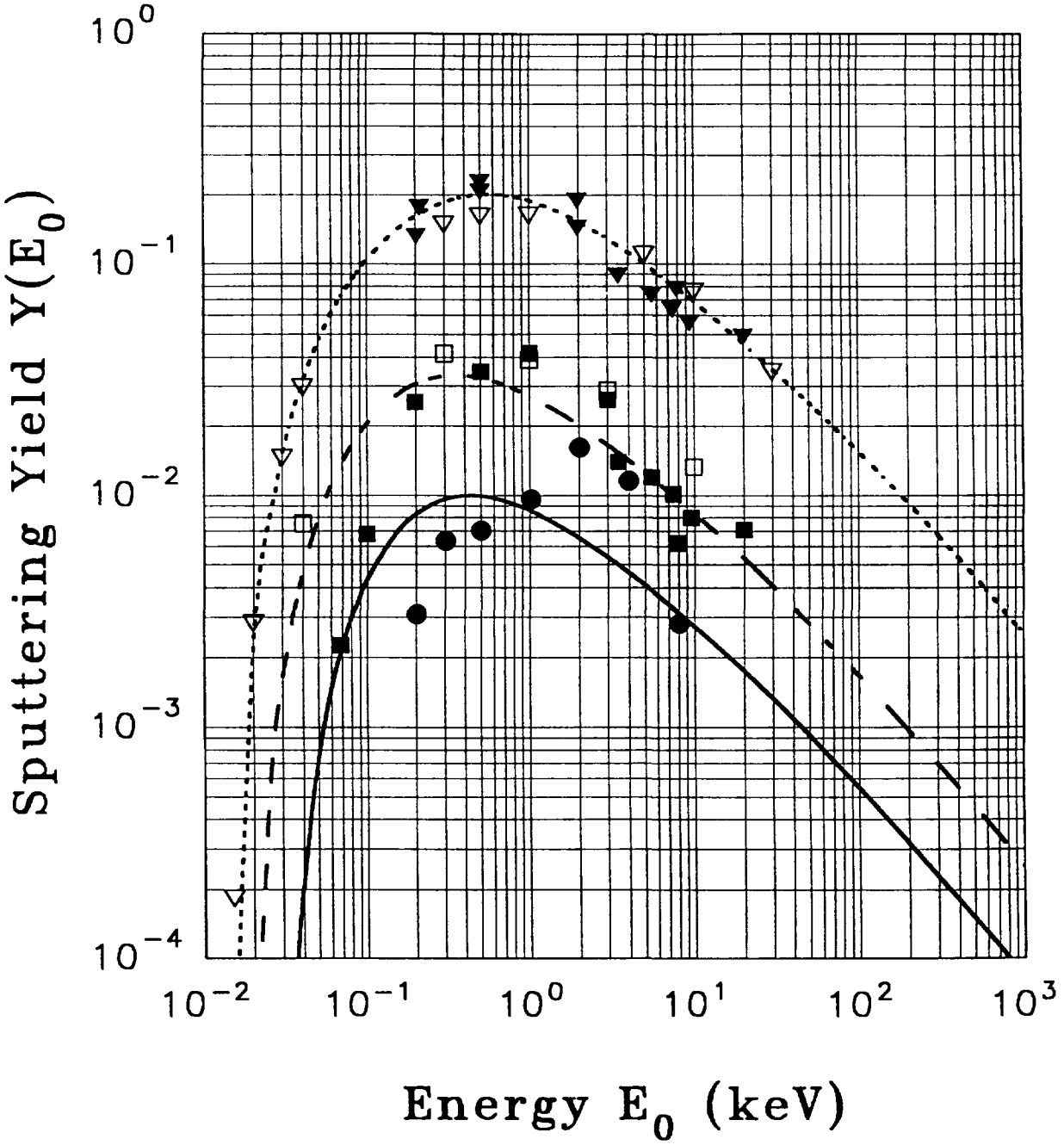

Fig. 9. Sputtering yield of Al for impact of He^+ (triangles, short dashed line), D^+ (squares, dashed line) and H^+ (circles, full line) as a function of energy in keV. Full symbols are experimental measurements from the work of the Garching group taken from the report by Matsunami et al [1] with supplementary information from Refs. [9] and [17]. The open symbols are TRIM simulation results from Refs. [9] and [17]. Lines are the results of the present fit of Eq. 11 with the values of α shown in Table 2.

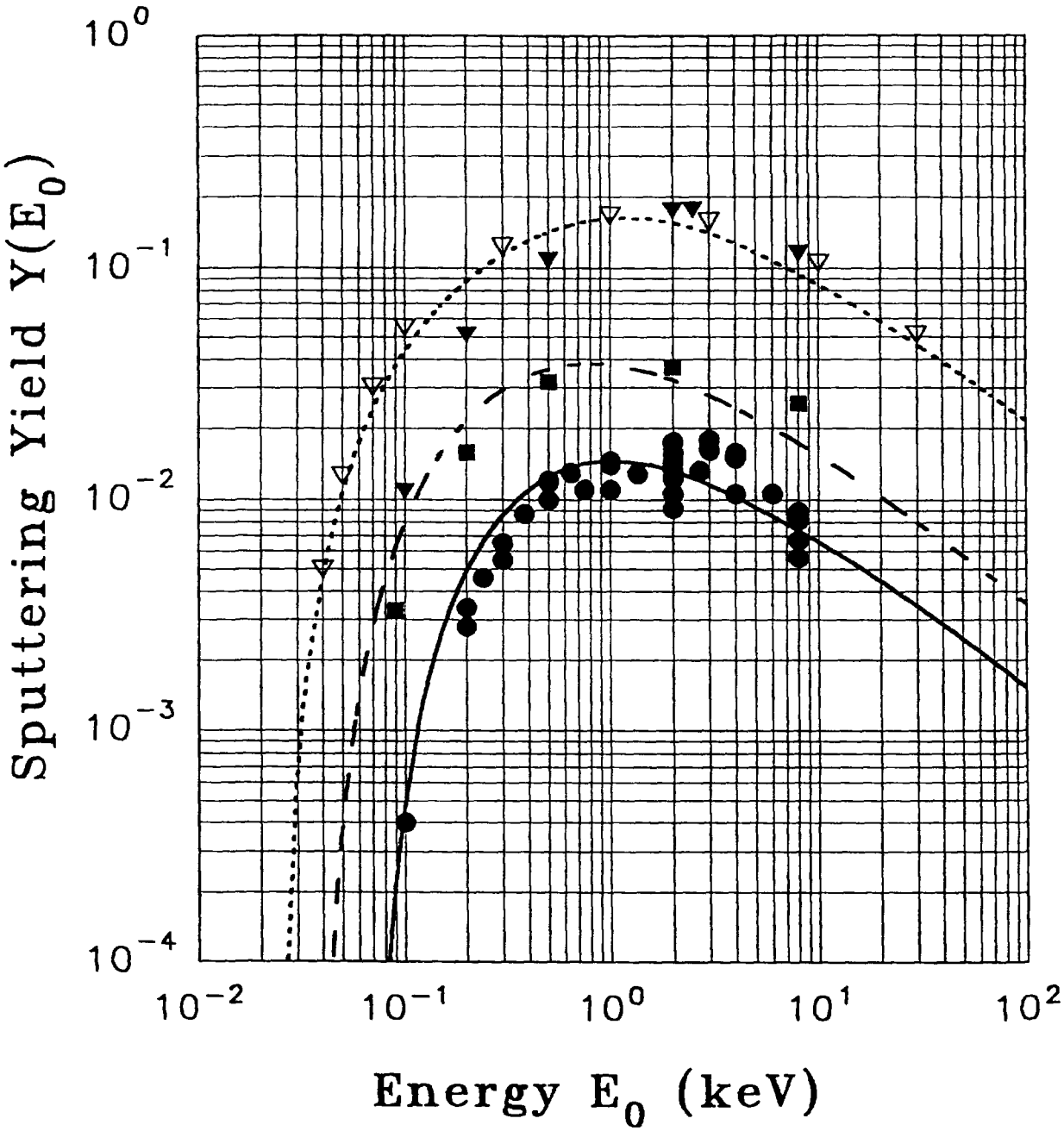

Fig. 10. Sputtering yield of Fe for impact of He^+ (triangles, short dashed line), D^+ (squares, dashed line) and H^+ (circles, full line) as a function of energy in keV. Full symbols are experimental measurements from the work of the Garching group taken from the report by Matsunami et al [1] with supplementary information from Refs. [9] and [17]. The open symbols are TRIM simulation results from Refs. [9] and [17]. Lines are the results of the present fit of Eq. 11 with the values of α shown in Table 2.

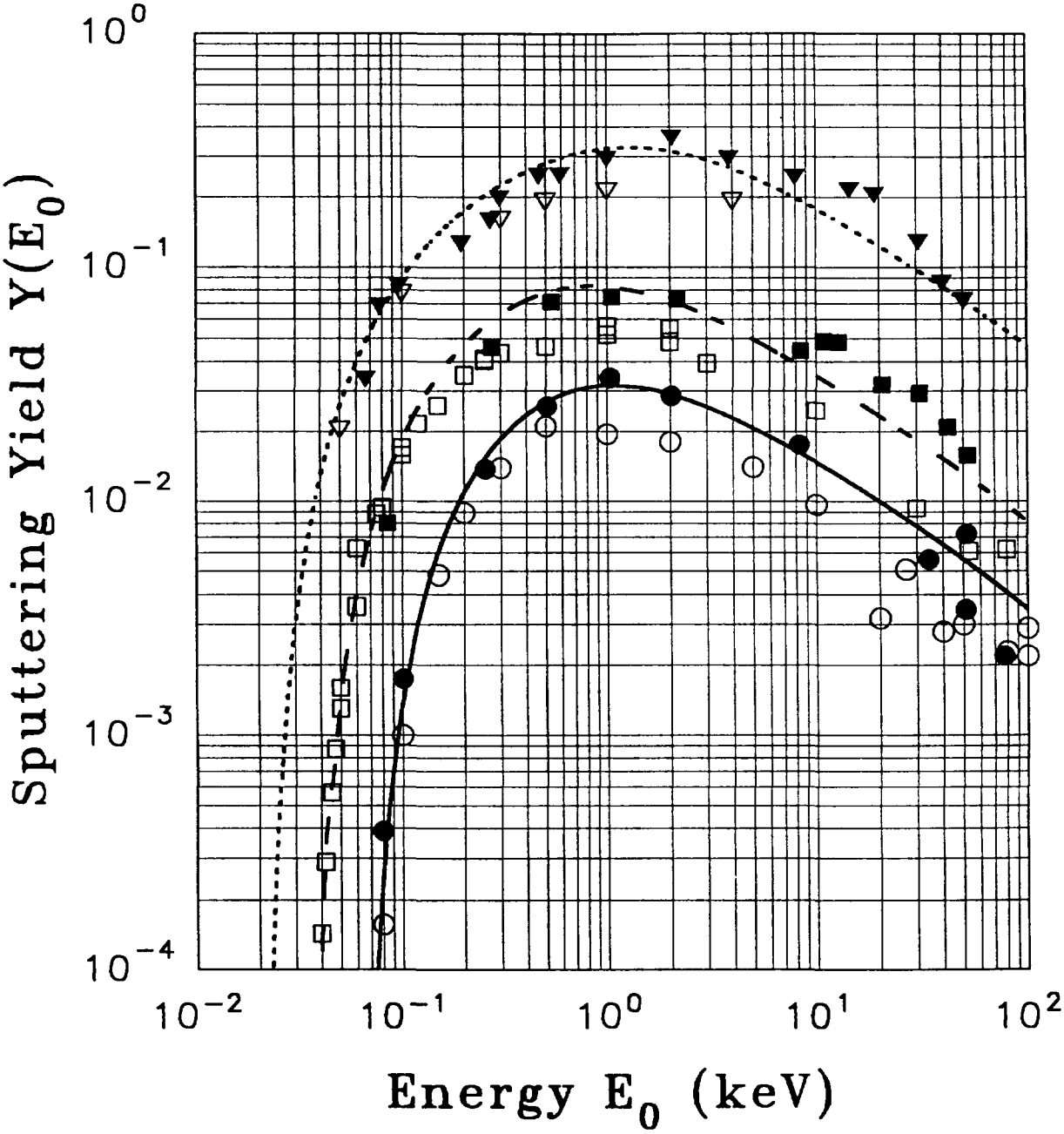

Fig. 11. Sputtering yield of Cu for impact of He^+ (triangles, short dashed line), D^+ (squares, dashed line) and H^+ (circles, full line) as a function of energy in keV. Full symbols are experimental measurements from the work of the Garching group taken from the report by Matsunami et al [1] with supplementary information from Refs. [9] and [17]. The open symbols are TRIM simulation results from Refs. [9] and [17]. Lines are the results of the present fit of Eq. 11 with the values of α shown in Table 2.

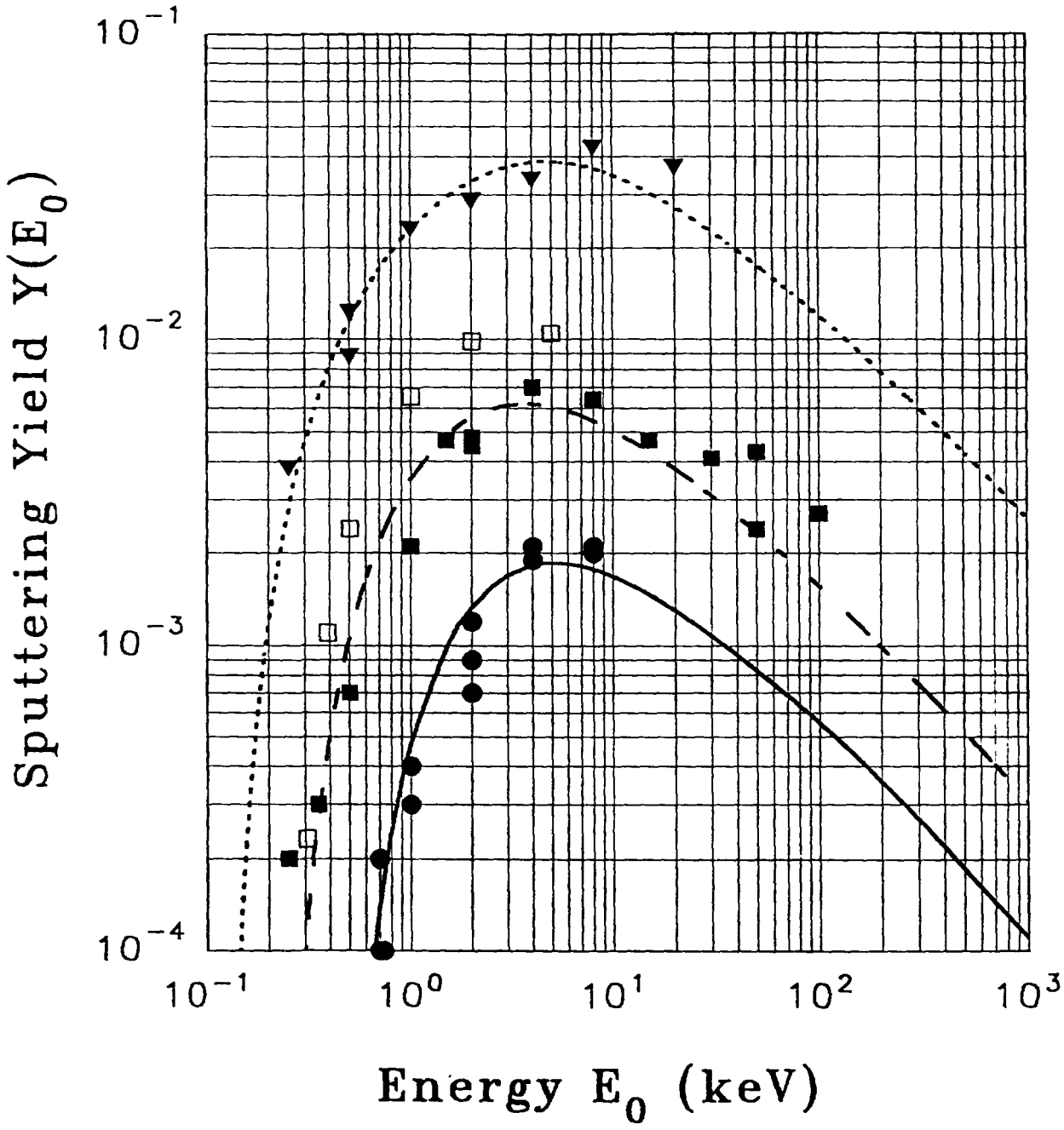

Fig. 12. Sputtering yield of W for impact of He^+ (triangles, short dashed line), D^+ (squares, dashed line) and H^+ (circles, full line) as a function of energy in keV. Full symbols are experimental measurements from the work of the Garching group taken from the report by Matsunami et al [1] with supplementary information from Refs. [9] and [17]. The open symbols are TRIM simulation results from Refs. [9] and [17]. Lines are the results of the present fit of Eq. 11 with the values of α shown in Table 2.

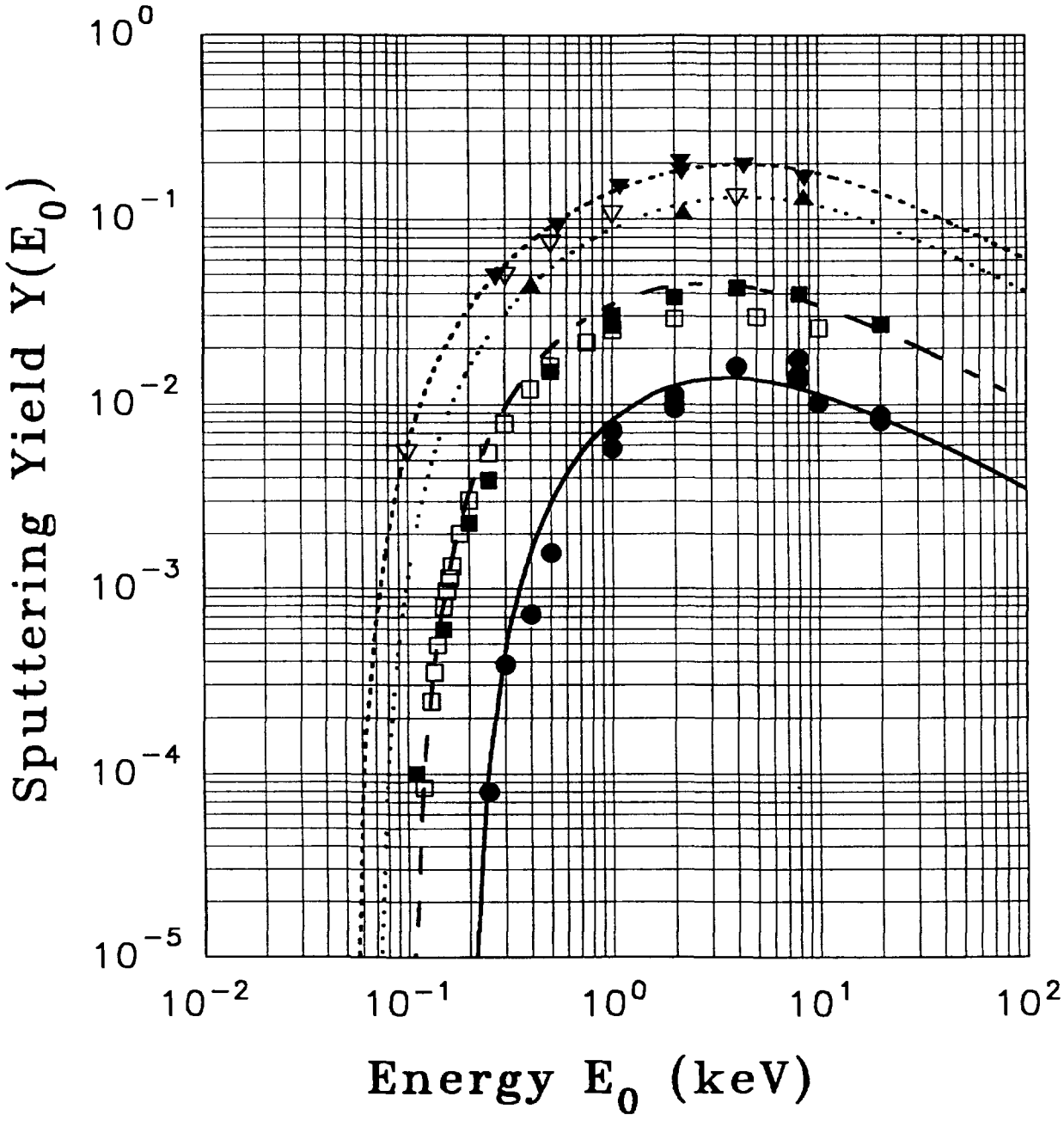

Fig. 13. Sputtering yield of Au for impact of He^+ (down triangles, short dashed line), $^3He^+$ (up triangles, dotted line), D^+ (squares, dashed line) and H^+ (circles, full line) as a function of energy in keV. Full symbols are experimental measurements from the work of the Garching group taken from the report by Matsunami et al [1] with supplementary information from Refs. [9] and [17]. The open symbols are TRIM simulation results from Refs. [9] and [17]. Lines are the results of the present fit of Eq. 11 with the values of α shown in Table 2.

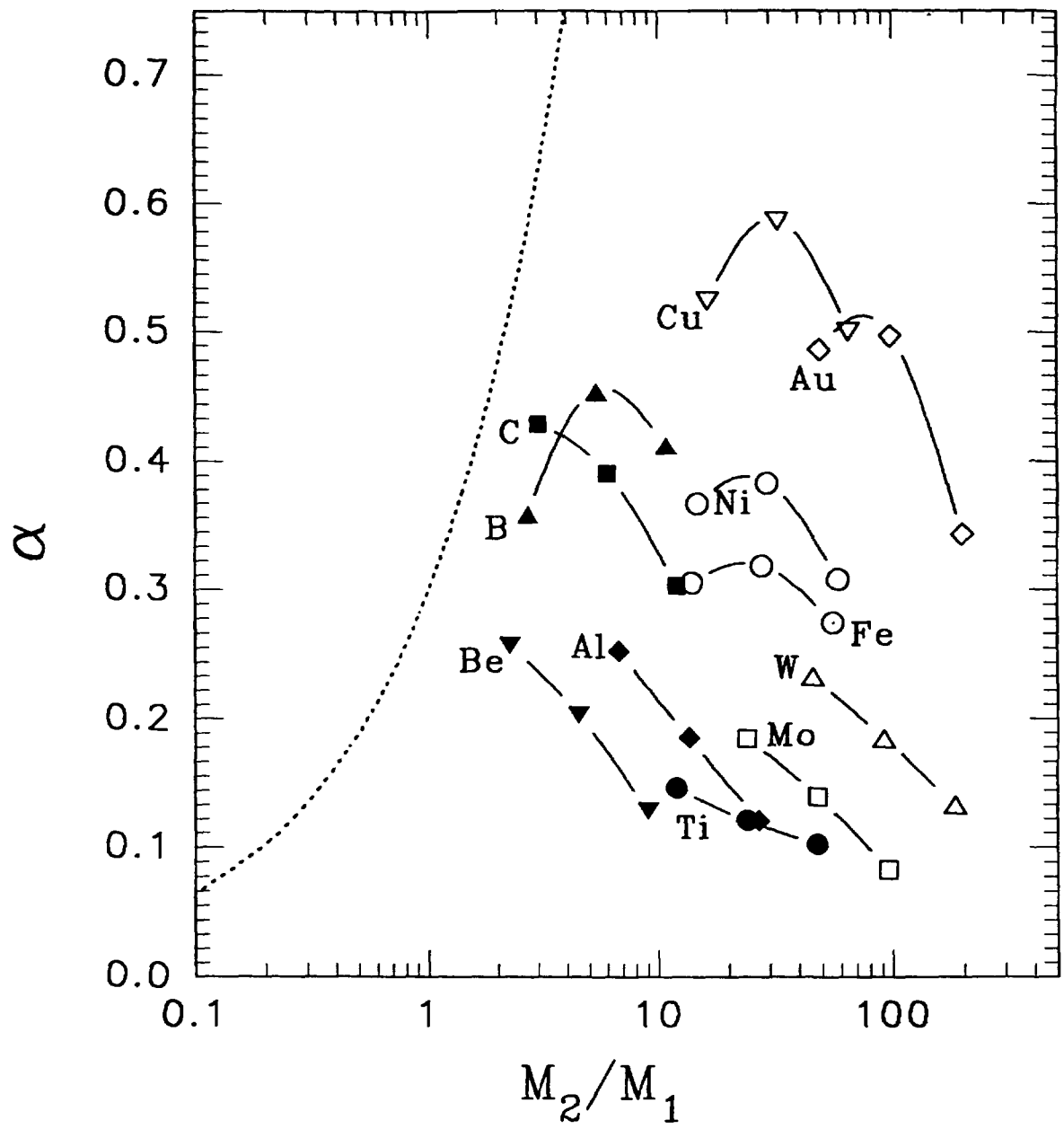

Fig. 14. Factor α from Eq. (2) shown as a function of target to projectile mass ratio M_2/M_1. The dashed line is a theoretical prediction derived from a model that is appropriate only to low mass ratios (say $M_2/M_1 < 1$) [10,11]). The solid lines are values of α from Table 2 and represent the values determined by the fitting of Eq. (12) to experimental data as described in the text. Lines are drawn through the data points for a particular target case only for the purpose of guiding the eye.

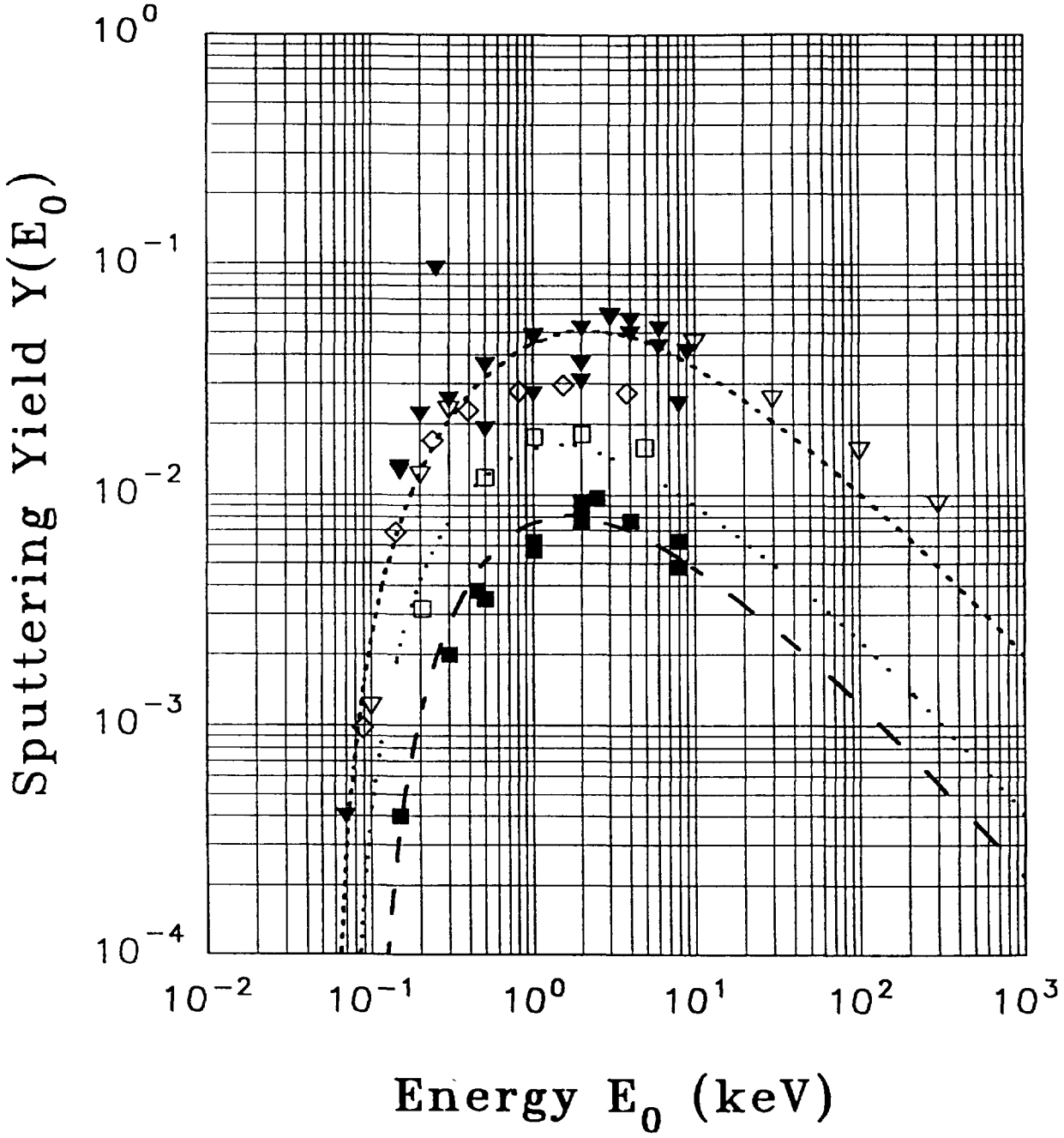

Fig. 15. Sputtering yield from Mo from impact of D^+ (long dashed curve, squares), T^+ (dotted curve, diamonds) and He^+ (dashed curve, triangles). Full symbols are from experiment, open symbols are simulation data [9,17]. The T^+ curve was obtained with α given by interpolating the corresponding curve in Fig. 14. Notice that the disagreement between the T^+ fit and the simulation data is similar to the disagreement between the simulation data (open squares) and experiment (full squares) for the case of D^+ (see text).

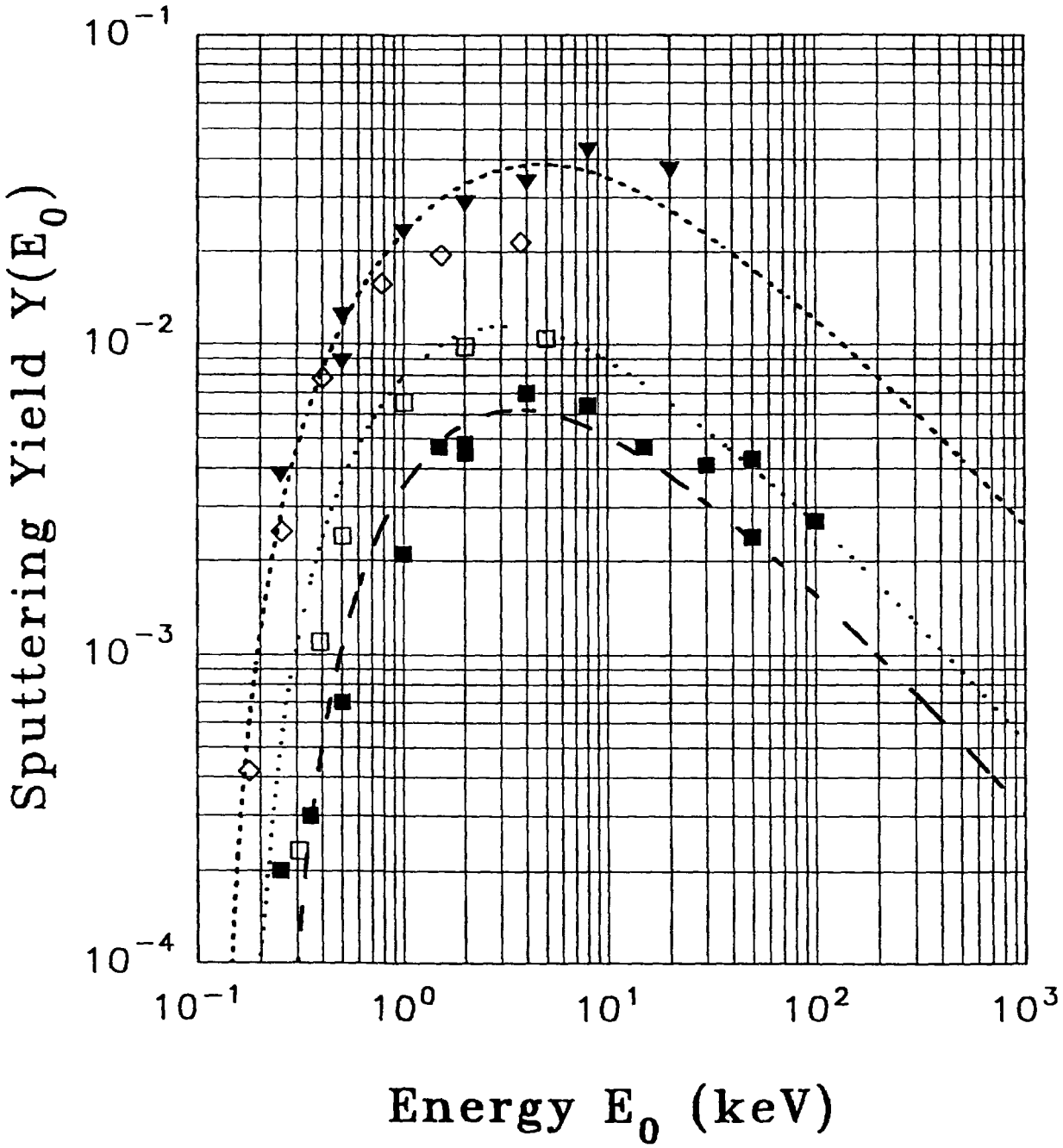

Fig. 16. Sputtering yield from W from impact of D^+ (long dashed curve, squares), T^+ (dotted curve, diamonds) and He^+ (dashed curve, triangles). Full symbols are from experiment, open symbols are simulation data [9,17]. The T^+ curve was obtained with α given by interpolating the corresponding curve in Fig. 14. Notice that the disagreement between the T^+ fit and the simulation data is similar to the disagreement between the simulation data (open squares) and experiment (full squares) for the case of D^+ (see text).

Abstract

Previously published data on physical sputtering of surfaces by light ions are critically reviewed with the aim of providing a single evaluated data set for a range of projectile-target combinations of interest to the modelling of plasma fusion device's first wall interactions. Experimental data often exhibits poor reliability and are not necessarily suitable for testing empirical formulae. Moreover, previously published empirical formulae are shown to be inconsistent with recent Monte-Carlo simulations. A revised set of formulae is suggested with empirical constants evaluated by comparison with the simulation data and is shown to be consistent with experiment. Fitting of the proposed formulae to an experimental data for a specific projectile target combination can be achieved with a single parameter

Reproduced by the IAEA in Austria
October 1993

93-03954